

State-Targeted Energy Projection: A Simple and Robust Approach to Orbital Relaxation of Non-Aufbau Self-Consistent Field Solutions

Kevin Carter-Fenk* and John M. Herbert*

Cite This: *J. Chem. Theory Comput.* 2020, 16, 5067–5082

Read Online

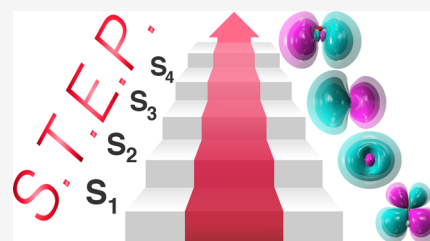
ACCESS |

Metrics & More

Article Recommendations

Supporting Information

ABSTRACT: Orbital optimization is crucial when using a non-Aufbau Slater determinant that involves promotion of an electron from a (nominally) occupied molecular orbital to an unoccupied one, or else ionization from a molecular orbital that lies below the highest occupied frontier molecular orbital. However, orbital relaxation of a non-Aufbau determinant risks “variational collapse” back to the Aufbau solution of the self-consistent field (SCF) equations. Algorithms such as the maximum overlap method (MOM) that are designed to avoid this collapse are not guaranteed to work, and more robust alternatives increase the cost per SCF iteration. Here, we introduce an alternative procedure called state-targeted energy projection (STEP) that is based on level shifting and is identical in cost to a normal SCF procedure, yet converges in numerous cases where MOM suffers variational collapse. Benchmark calculations on small-molecule reference data suggest that Δ SCF calculations based on STEP are an accurate way to compute both ionization and excitation energies, including core-level ionization and excited states with significant double-excitation character. For the molecule 2,4,6-trifluoroborazine, Δ SCF calculations based on STEP afford excellent agreement with experiment for both vertical and adiabatic ionization energies, the latter requiring geometry optimization of a non-Aufbau valence hole. Semiquantitative agreement with experiment is obtained for the absorption spectrum of chlorophyll *a*. Finally, the importance of asymptotic exchange and correlation is illustrated by application to Rydberg states using spin-scaled Møller–Plesset perturbation theory with a non-Aufbau reference determinant. Together, these results suggest that STEP offers a reliable and affordable alternative to the MOM procedure for determining non-Aufbau solutions of the SCF equations.



I. INTRODUCTION

The Aufbau principle is a basic tenet of ground-state electronic structure theory, but many chemical properties such as ionization energies and electronic excitation energies can be viewed, conceptually at least, as non-Aufbau solutions to the electronic structure problem.^{1–4} For these solutions, occupancies of the molecular orbitals (MOs) are not so trivially assigned. Understanding non-Aufbau electronic configurations is essential in making contact with photoelectron spectroscopy, which readily probes electron removal below the highest occupied MO (HOMO), but perhaps also in understanding excited states that conserve the number of electrons. Especially in solid-state materials, the non-Aufbau determinantal picture may be more consistent with the “excitonic” (electron/hole or quasiparticle) concept of excited states, which is to be contrasted with the molecular spectroscopy viewpoint based on term symbols. To be quantitative, however, that excitonic picture requires orbital optimization in the excited state, since the canonical MOs are optimized for the ground state.

Single-reference computational tools for the study of electronically excited states include the configuration-interaction singles (CIS) method^{5–7} and time-dependent density functional theory^{7–11} (TD-DFT) within the linear-response approximation.^{12,13} Linear-response TD-DFT is certainly the most widely used quantum chemistry method for excited states, with a computational cost that scales formally as

$n_{\text{states}} \times O(n_{\text{basis}}^4)$,¹⁴ although often better than that in practice.^{15,16} By including electron correlation effects that are lacking in the CIS approach, TD-DFT often achieves a statistical accuracy of 0.2–0.3 eV for vertical excitation energies,¹⁷ although certain systemic problems remain.^{18–35} For spatially localized excitations, both CIS and TD-DFT can be considered to include some effects of orbital relaxation in the excited state, as the single-excitation *ansatz* is equivalent to a variationally optimized orbital rotation. This orbital relaxation neglects correlation in the CIS case and neglects long-range exchange and correlation in semilocal DFT approaches, with the result that orbital relaxation effects vanish for long-range charge-transfer excitations. In the CIS case, promotion of a single electron between well-separated donor and acceptor orbitals leaves no remaining excitations to relax the orbitals, with the effect that CIS calculations systematically overestimate charge-transfer excitation energies by 1–2 eV.³⁶ Systematic *underestimation* of charge-transfer energies by TD-DFT is well-documented.^{18–28}

Received: May 16, 2020

Published: July 9, 2020



In the CIS case, this can be ameliorated by explicit orbital optimization,³⁷ and density relaxation (i.e., of the occupied–virtual block of the excited-state density matrix¹²) is also important in TD-DFT.^{38,39}

One of the simplest procedures to incorporate electronic relaxation into self-consistent field (SCF) electronic structure methods is to use a “ Δ SCF” protocol in which a non-Aufbau determinant is optimized directly and the excitation or ionization energy is computed as the energy difference with respect to the original ground-state determinant. (This remains the dominant paradigm to compute excitation energies in solids,^{40–43} because periodic DFT with semilocal functionals is fundamentally ill-posed.^{44,45}) The difficulty with such a procedure is that any non-Aufbau solution to the SCF equations is at best a local (not global) minimum of the SCF Lagrangian, and often such solutions are actually saddle points rather than minima. As such, it is relatively easy for a non-Aufbau solution to undergo “variational collapse” to the ground-state solution.

Methods that attempt to use SCF-like equations to compute single-determinant approximations to excited-state wave functions have a long history in quantum chemistry,^{46–49} having first been introduced in the form of various “improved virtual orbital” techniques,^{46–51} also known as extended Hartree–Fock theory.⁴⁹ More recently, methods have been developed that seek to elucidate most or all solutions to the SCF equations for a given system.^{52–55} This may hold utility as a basis for configuration interaction,^{54–56} but represents considerable overkill for most practical applications.

The maximum overlap method (MOM),^{1,4} on the other hand, is a simple procedure designed to locate a particular non-Aufbau solution to the SCF equations, based on similarity to a user-defined set of orbitals. The MOM procedure attempts to avoid variational collapse by selecting the occupied MOs at each SCF iteration based on their overlap with a set of reference orbitals, an approach that is formally simple, conceptually appealing, and introduces only a small additional overhead on top of the usual cost per SCF iteration. This approach is considerably simpler than alternatives based on constrained variation^{57–76} or modified variational principles,^{77–82} and that simplicity facilitates the use of ground-state machinery to compute energy gradients and properties. The non-Aufbau SCF solutions obtained using MOM are generally not orthogonal to the ground-state determinant, a fact that has consequences for properties such as oscillator strengths,⁶⁵ although often the optimized excited-state determinants are *nearly* orthogonal to the SCF ground state.¹ In any case, tests on simple systems such as excited states of He atom² and H₂ molecule³ generally support the identification of these non-Aufbau solutions with genuine excited states of the systems in question. The MOM-based Δ SCF procedure has been used to compute valence excitation energies^{1–4,83–88} as well as excited-state geometries and vibrational frequencies.^{89–93} Core-level excitation energies^{94–99} and ionization energies^{100–105} have been computed in the same way, and core-hole states obtained via the MOM procedure have been used as reference states for an excited-state calculation of valence-to-core emission spectra.^{106–113}

Although MOM provides a well-defined algorithm for which orbitals to occupy, it does not specify the SCF convergence procedure; various direct-minimization algorithms either have been or could be used in conjunction with MOM.^{86,114–116} Direct minimization is usually a better choice in this context as compared to extrapolation procedures such as direct inversion in the iterative subspace (and variants thereof),¹¹⁷ as extrapolative

algorithms often lead to variational collapse. Even with direct minimization, however, the MOM-SCF procedure is not immune to variational collapse, sometimes rendering the desired non-Aufbau state unobtainable in practice.¹¹⁸ For such cases, an alternative Δ SCF procedure would be desirable.

One such alternative is squared-gradient minimization (SGM),¹¹⁹ in which the square of the orbital gradient is optimized rather than the energy Lagrangian itself, thereby converting a saddle-point optimization into a proper minimization. This makes SGM exceptionally robust against variational collapse, although it is 2–3 \times more expensive (per iteration) as compared to a conventional SCF algorithm, depending on the availability of analytic orbital Hessians.¹¹⁹ (SGM-DFT is 2 \times more expensive than MOM-DFT if the functional derivative $\delta^2 E_{xc}/\delta\rho^2$ is available, otherwise it is 3 \times more expensive.¹¹⁹)

In this work, we present a new Δ SCF approach based on level shifting, which has the same cost per cycle as a conventional SCF procedure but is considerably more robust as compared to MOM-SCF. This method is benchmarked against accurate theoretical values for small-molecule excitation energies, including some doubly excited states. The cost-effective nature of the procedure is demonstrated by optimizing the nuclear geometry of valence-hole states, in order to compute the adiabatic ionization spectrum of 2,4,6-trifluoroborazine. Finally, we apply the new procedure to analyze the photoactive chlorin center in chlorophyll *a*.

II. THEORY

In what follows, indices i, j, k, \dots refer to occupied MOs in the ground-state Slater determinant, whereas a, b, c, \dots refer to virtual MOs and r, s, t, \dots are arbitrary MOs. Atomic orbital (AO) basis functions are indicated with Greek indices μ, ν, λ, \dots . For simplicity, all equations are written in closed-shell form, but the extension to spin-unrestricted orbitals is straightforward and has been implemented as well. To put our work in context, we first review the MOM approach (in Section II.A) and the SGM method (in Section II.B). Our new approach, state-targeted energy projection (STEP), is introduced in Section II.C. Finally, we discuss approximate spin-purification procedures (for single-determinant approximations to open-shell singlet wave functions) in Section II.D.

II.A. Maximum Overlap Method (MOM). Upon diagonalizing the Fock matrix to obtain a set of MOs at the current SCF iteration, one must decide which of these MOs to choose as the occupied ones. The MOM-SCF procedure¹ is probably the most popular approach for obtaining non-Aufbau solutions to the SCF equations, and it selects the occupied MOs as the ones having maximum overlap with the occupied MOs in the previous SCF iteration. To do this, one computes normed projections

$$p_r = \left(\sum_i^{\text{occ}} \langle \psi_i^{(n-1)} | \psi_r^{(n)} \rangle^2 \right)^{1/2} \quad (1)$$

where $\{\psi_r^{(n)}\}$ are the MOs at the current iteration, n . The new occupied MOs are selected to be the ones with the largest projections p_r .

The original MOM procedure can sometimes result in drift of the reference orbitals $\{\psi_r^{(n)}\}$ away from the non-Aufbau state of interest, sometimes leading to variational collapse.¹¹⁸ An alternative is the “initial MOM” (IMOM) procedure,⁴ where the projection that is computed is instead

$$p_r = \left(\sum_i^{\text{occ}} \langle \psi_i^{(0)} | \psi_r^{(n)} \rangle^2 \right)^{1/2} \quad (2)$$

This anchors the projection to an initial set of occupied MOs, $\{\psi_i^{(0)}\}$. As compared to the original MOM-SCF procedure, IMOM-SCF tends to have better success converging the non-Aufbau state of interest, although it is not infallible.¹¹⁹

II.B. Squared-Gradient Minimization (SGM). Minimization of the squared potential energy gradient $\|\hat{\nabla}V(\mathbf{x})\|^2$ is a known trick to turn transition-state optimization into a minimization problem,^{120–123} and SGM in the space of orbital rotations was recently introduced as a more robust alternative to MOM.¹¹⁹ Rather than using the potential energy $V(\mathbf{x})$, this method optimizes an objective function Δ equal to the squared-gradient of a Lagrangian, \mathcal{L} :

$$\Delta(\theta) \equiv \|\hat{\nabla}_\theta \mathcal{L}\|^2 = \sum_{ai} \left| \frac{\partial \mathcal{L}}{\partial \theta_{ai}} \right|^2 \quad (3)$$

The variables θ_{ai} represent orbital degrees of freedom. For SCF levels of theory, \mathcal{L} is simply the single-determinant energy with Lagrange multiplier constraints to enforce orbital orthogonality, as in the usual derivation of the SCF equations.¹²⁴ Minimization of $\Delta(\theta)$ turns saddle-point optimization into a search for a true minimum, making SGM an exceptionally robust way to optimize a single-determinant approximation to an excited-state wave function. That said, it is known that the $\|\hat{\nabla}V(\mathbf{x})\|^2$ surface contains spurious minima that do not correspond to stationary points on the potential energy surface $V(\mathbf{x})$,^{121–123,125} and it is therefore conceivable that orbital-based SGM could converge to a state having no physical significance.

Nevertheless, in the context of SCF methods, the SGM algorithm does appear to be less susceptible to variational collapse as compared to MOM or IMOM.¹¹⁹ The trade-off for this improved robustness, however, is that SGM is less efficient per SCF iteration, because calculation of the gradient $\partial\Delta/\partial\theta_{ai}$ for mean-field methods costs twice as much as a standard Fock build.¹¹⁹ (A more general, finite-difference optimization procedure requires three Fock builds per SCF cycle.¹¹⁹) This may limit the applicability for larger molecules, especially for geometry optimizations.

II.C. State-Targeted Energy Projection (STEP). The STEP algorithm introduced here represents an attempt to marry the robustness of SGM with the efficiency of MOM. In order to target the desired states, the STEP algorithm employs constraints in the form of a level shift to the energies of the virtual MOs. Level-shifting, which has the effect of restricting occupied–virtual rotations, has been used in the past to facilitate SCF convergence,¹²⁶ especially in cases of degenerate or near-degenerate frontier orbitals. In such instances, the level shift functions to separate the lowest unoccupied MO (LUMO) from the quasi-degenerate HOMO, such that an Aufbau selection of the occupied MOs is more likely to generate a consistent set of occupied MOs at each SCF iteration, eliminating undesirable oscillations that hamper convergence. Here, we use the concept of the level shift to constrain the Fock matrix, placing restrictions on the allowed occupied–virtual rotations in order to facilitate convergence to a saddle-point solution.

Consider the projection operator

$$\hat{Q} = \sum_a^{\text{virt}} |\psi_a\rangle\langle\psi_a| \quad (4)$$

onto the virtual space. In the AO basis, the projector in eq 4 is

$$\begin{aligned} \hat{Q} &= \sum_{\mu\nu} \sum_a^{\text{virt}} |\mu\rangle C_{\mu a} C_{\nu a}^* \langle\nu| \\ &= \sum_{\mu\nu} |\mu\rangle Q_{\mu\nu} \langle\nu| \end{aligned} \quad (5)$$

where the matrix \mathbf{Q} is the virtual block of \mathbf{CC}^\dagger . Taking matrix elements in the AO basis, we arrive at a level shift for the virtual space. Adding this to the Fock matrix \mathbf{F} results in a modified Fock matrix

$$\mathbf{F}' = \mathbf{F} + \eta \mathbf{SQS} \quad (6)$$

where η is a parameter. The action of the level shift $\eta\mathbf{SQS}$ is to elevate the energy of orbital ψ_a from ε_a to $\varepsilon_a + \eta$, for each ψ_a that is contained in the summation of eq 4. Note that the level-shift operator \mathbf{SQS} in eq 6 represents the orthogonal complement of the AO-based level shift that is applied in the more typical context of SCF convergence.¹²⁷

For the applications of interest, we assume that we are given a set of non-Aufbau MOs, such that at least one virtual energy level $\varepsilon_{a'}$ lies below the HOMO level, $\varepsilon_{a'} < \varepsilon_{\text{HOMO}}$. Initially (in the first SCF iteration), this may simply constitute a relabeling of the MOs. For example, we might promote an electron from the HOMO – 1 to the LUMO + 1 and then designate $\psi_{\text{HOMO}-1}$ as virtual and $\psi_{\text{LUMO}+1}$ as occupied. A sufficiently large shift of the virtual orbital energy levels will elevate $\varepsilon_{a'}$ above the eigenvalues ε_i that represent occupied levels, so that the desired electron configuration is obtained by Aufbau occupation of the MOs obtained by diagonalizing the modified Fock matrix \mathbf{F}' in eq 6.

Mathematically, a very large level shift is appealing because it forces the changes between SCF cycles to be arbitrarily small, such that the SCF procedure will always converge to a nearby stationary point.^{128,129} In practice, however, a level shift that is too large will significantly restrict the occupied–virtual rotations, leading to very slow SCF convergence. In an effort to choose the smallest level shift that retains the desired electron configuration, we anchor the shift to the HOMO/LUMO gap and set

$$\eta = |\varepsilon_{\text{HOMO}} - \varepsilon_{\text{LUMO}}| + \epsilon' \quad (7)$$

where ϵ' is a small empirical parameter. This choice is reminiscent of the level shift that is applied in the trust-region SCF method.¹³⁰ If we were to set $\epsilon' = 0$ in eq 7, then for a valence- or core-hole state with $\varepsilon_{\text{LUMO}} < \varepsilon_{\text{HOMO}}$ the HOMO and LUMO energies would be level-shifted into degeneracy with one another. The purpose of the parameter ϵ' is to avoid this situation, ensuring the desired occupation at each SCF cycle. We find that $\epsilon' = 0.1$ Ha is sufficient to avoid variational collapse without significantly increasing the number of SCF iterations beyond what is typical for a ground-state orbital optimization. In any case, ϵ' controls the strictness of the level-shift constraint. A sufficiently large value of ϵ' will guarantee convergence to the nearest solution of the SCF equations but potentially at the price of a larger number of SCF iterations required for convergence. The value of η is determined only once, using the initial non-Aufbau set of orbitals.

The STEP procedure is illustrated in Figure 1, highlighting the role of $\eta\mathbf{SQS}$. Starting from a set of initial guess orbitals and

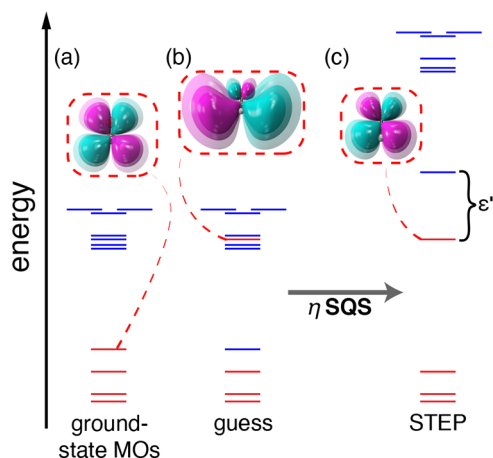


Figure 1. STEP protocol begins with (a) a set of initial MOs, probably the Aufbau-occupied set from some previous calculation. In (b), a nominal virtual MO is selected to be part of a non-Aufbau occupied set, and then (c) this initial guess is relaxed using a level shift, where the parameter ϵ' ensures the desired occupation. In each panel, the occupied levels are shown in red, and the virtual levels are shown in blue.

occupancies, the STEP algorithm relaxes the MOs under the constraint that the Aufbau principle satisfies the desired occupancy criteria (not just the ground-state occupation) throughout orbital optimization. The effects of MO relaxation can be large, as shown qualitatively in the difference between the unrelaxed π^* orbital that is selected for occupancy in Figure 1b, as compared to its fully relaxed progeny that is shown following STEP-SCF convergence in Figure 1c.

While the initial guess can usually be constructed using the ground-state MOs, level shifting ensures convergence to the nearest stationary point. This makes the STEP-SCF procedure more dependent on the initial guess than MOM-SCF. In instances where the desired state cannot be optimized, it might be necessary to use a set of excited-state MOs as an initial guess, e.g., natural transition orbitals¹³¹ (equivalent to CIS natural orbitals).¹³² That said, all of the calculations reported in this work use ground-state unrestricted Hartree–Fock (UHF) or unrestricted Kohn–Sham (UKS) MOs to construct the initial-guess occupancies.

II.D. Spin Purification. Excited states are generally open-shell, and thus single-determinant approximations to them are inherently spin-contaminated, often badly so. For single-determinant approximations to open-shell singlets, it is not unusual to obtain $\langle \hat{S}^2 \rangle \approx 1$ (in atomic units), representing the average of singlet and triplet values, similar to (and for the same reason as) the UHF wave function in the dissociation limit.¹²⁴ Nevertheless, Δ SCF excitation energies for open-shell singlets are often surprisingly accurate despite the spin contamination.^{1,4,83} In certain cases, such as the $^1B_{1u}$ state of C_2H_4 , spin contamination leads to severe underestimation of the excitation energy.¹

We will test a simple spin-purification scheme for open-shell singlet excited states based on the multiplet splitting formula^{133,134}

$$E_{\text{sing}} \approx 2E_{\text{mix}} - E_{\text{trip}} \quad (8)$$

in which the spin-purified singlet energy E_{sing} is approximated using the “mixed-spin” (spin-contaminated singlet) energy, E_{mix} , along with the high-spin triplet energy, E_{trip} . This formula can be

viewed as an approximate form of spin projection.^{135–137} While eq 8 has occasionally been implemented self-consistently,¹³⁸ for Δ SCF calculations it is typically used as a *posteriori* correction,^{87–91,139–141} taking E_{mix} to be the single-determinant energy obtained for the singlet excited state in question. (This is sometimes called the “broken symmetry” solution.¹³⁶) For the $^1B_{1u}$ state of C_2H_4 , use of eq 8 reduces the Δ SCF error obtained with the B3LYP functional from 1.8 to 0.3 eV.¹

In the present work, we will compare spin-purified Δ SCF excitation energies ($\Delta E = E_{\text{sing}} - E_0$) to results without spin purification ($\Delta E = E_{\text{mix}} - E_0$), in an effort to test the limits of the single-determinant model. Spin purification is applied to the Δ SCF results only and not to results based on second-order Møller–Plesset perturbation theory (MP2), as spin-projection for MP2 wave functions is more involved.¹⁴²

III. RESULTS AND DISCUSSION

We have implemented the STEP algorithm in a locally modified version of Q-Chem,¹⁴³ which contains the MOM, IMOM, and SGM algorithms as well and was used for all calculations reported here.

III.A. Convergence Studies. Variational collapse to a lower-energy state is a possibility in any Δ SCF method, so it is important to understand the limitations of any given algorithm when it comes to optimizing a non-Aufbau determinant. We first examine convergence properties for excited states of some very simple systems: boron atom, formaldehyde, and nitrobenzene. Excited-state calculations on boron and formaldehyde were carried out at the UHF/aug-cc-pVTZ level, whereas we describe nitrobenzene at the UHF/def2-TZVP level for consistency with a published convergence study using SGM.¹¹⁹ The SCF convergence threshold was set to a root mean squared (RMS) error of 10^{-8} Ha for all calculations reported in this section.

Results in Figure 2 show convergence of the 2^2P state of boron atom that is obtained by $2p_x \rightarrow 3p_y$ excitation. Results are shown

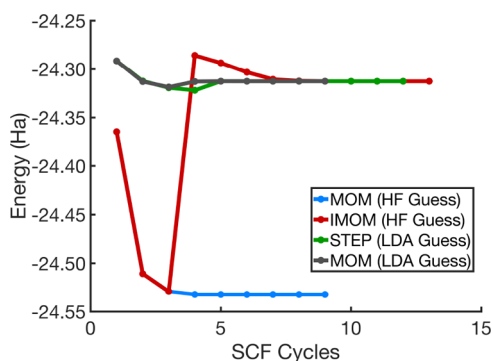


Figure 2. Convergence of the 2^2P ($2p_x \rightarrow 3p_y$) state of boron using various orbital optimization algorithms. Each algorithm starts with non-Aufbau initial-guess orbitals from either a UHF or a UKS calculation of the ground state, and then iterations proceed at the UHF/aug-cc-pVTZ level in either case.

for MOM, IMOM, and STEP; all three algorithms are capable of converging to the final 2^2P state, albeit under different initial guess conditions. In this example, the use of non-Aufbau UHF orbitals as the initial guess causes both MOM and STEP to collapse to the ground state. The failure of STEP in this particular instance occurs because the first Roothaan step with the non-Aufbau UHF orbitals produces a new set of orbitals with an Aufbau configuration. The resulting form of F' in eq 6 then

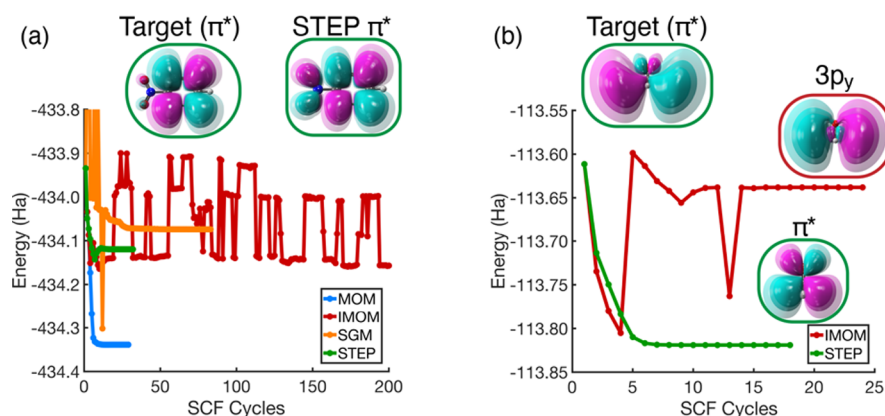


Figure 3. Convergence behavior in two cases that prove challenging for MOM-based SCF methods: (a) $n_{\pi} \rightarrow \pi^*$ transition of nitrobenzene described at the UHF/def2-TZVP level, where MOM suffers variational collapse and IMOM oscillates between different sets of orbitals, and (b) $n \rightarrow \pi^*$ transition of formaldehyde described at the UHF/aug-cc-pVTZ level as the excitation from orbital 8 to orbital 11 ($\psi_8^{\beta} \rightarrow \psi_{11}^{\beta}$), where IMOM converges to the wrong state. The inset figures show the π^* orbital before (“target”) and after (“STEP”) optimization. Also shown in (b) is the final $3p_y$ orbital to which the IMOM-SCF algorithm converges.

leads to a solution that is trivially Aufbau (i.e., the $\eta = 0$ solution is equivalent to all solutions with $\eta > 0$), causing STEP to converge to the ground-state solution. This collapse can be circumvented by initializing STEP using ground-state UKS orbitals from the local density approximation (LDA) as the initial guess for a subsequent calculation at the UHF level. Similar convergence problems occasionally emerge with SGM (though not in the case of boron) when $\hat{V}_{\theta}\Delta = 0$ due to the presence of a Coulson-Fischer point.¹¹⁹ Although the cause of the convergence difficulty is different, Hait and Head-Gordon sidestep problematic cases by seeding SGM with LDA orbitals,¹¹⁹ as we have done here with STEP.

The MOM procedure also suffers variational collapse to the ground state when seeded with UHF initial-guess orbitals but succeeds in finding the 2^2P state when initialized using LDA orbitals. Both STEP and MOM require a set of initial guess orbitals that lie within the basin of attraction of the desired state, implying that the initial non-Aufbau UHF orbitals are in fact more similar to the Aufbau (ground-state) solution than they are to the 2^2P state. In contrast to the MOM algorithm that collapses to the ground state, IMOM escapes the initial Aufbau configuration generated by the UHF guess by switching occupancies between cycles 3 and 4, as seen by the large, abrupt change in the energy in Figure 2.

While the outcome of a calculation starting from $2p_x \rightarrow 3p_y$ promotion depends sensitively on the nature of the initial guess, it is worth noting that STEP easily converges the degenerate $2p_x \rightarrow 3p_x$ excitation. That said, the STEP algorithm, much more so than MOM, requires a qualitatively correct set of occupied orbitals at the outset.

Although this dependence on the initial guess may seem undesirable, it does allow STEP to succeed in cases where MOM-based algorithms fail. Two such cases are shown in Figure 3, where we investigate the lowest $n \rightarrow \pi^*$ transitions in nitrobenzene and formaldehyde. For nitrobenzene (Figure 3a), the IMOM-SCF algorithm oscillates for over 500 cycles as it switches between two sets of orbitals, whereas MOM-SCF quickly collapses to the ground state. Guaranteed retention of the original guess occupancies in STEP, however, allows this method to converge to the correct state in only 32 cycles, which means 32 Fock builds. This example was considered previously using SGM,¹¹⁹ and the same state was successfully optimized but

only after 83 SCF cycles (using the same convergence criterion), meaning 166 Fock builds.

Notably, the STEP algorithm converges the $n\pi^*$ state of nitrobenzene to an energy of -434.11957288 Ha, as compared to -434.07387331 Ha using SGM, which makes for a difference of 1.4 eV between the two Δ SCF excitation energies. Furthermore, the n_{π} lone pair orbital remains unoccupied throughout the STEP procedure but actually becomes reoccupied during the SGM optimization (see Figure S1), so that even though SGM does not collapse to the ground state, it appears to converge to a different stationary point. This solution is minimum on the squared-gradient surface [as indicated by $\Delta(\theta) = 0$ at convergence] that does not coincide with a minimum on the potential energy surface. In the case of this very difficult excitation, STEP is the only algorithm that converges to the correct final state. It is possible that SGM might be made to converge to the correct state by taking smaller steps, as suggested by Hait and Head-Gordon,¹¹⁹ although this would come at the expense of additional iterations. In the SGM calculations presented here, we use a scaling factor $c = 1$ in the quasi-Newton update of the Hessian, as suggested in ref 119.

For the $n \rightarrow \pi^*$ state of formaldehyde (Figure 3b), the IMOM-SCF algorithm fails to converge to the correct state, converging instead to a different excited-state solution. This algorithm swaps orbitals in a manner similar to what was observed for the 2^2P of boron, and the final state that is optimized for H_2CO is best described as the $n \rightarrow 3p$ Rydberg state. In contrast, STEP-SCF optimizes the correct $n\pi^*$ state in just 18 iterations. The difference is that the occupancies cannot change abruptly in STEP as they can in (I)MOM, and instead the occupied MOs must be deformed continuously starting from the initial set. Although this potentially makes STEP more sensitive to the initial guess, it also means that the algorithm succeeds in difficult cases where MOM-based approaches are oscillatory or even converge to the wrong state. The STEP algorithm also succeeds in at least one case where the robust SGM algorithm converges to a state that is different from the one targeted by the initial-guess orbitals.

III.B. Formaldehyde Excitation Spectrum. Formaldehyde has a well-characterized excitation spectrum and is therefore an excellent benchmark for new methods. We consider 11 different excited states of H_2CO , comprising 5 singlets and 6 triplets and including both valence and Rydberg excitations. We

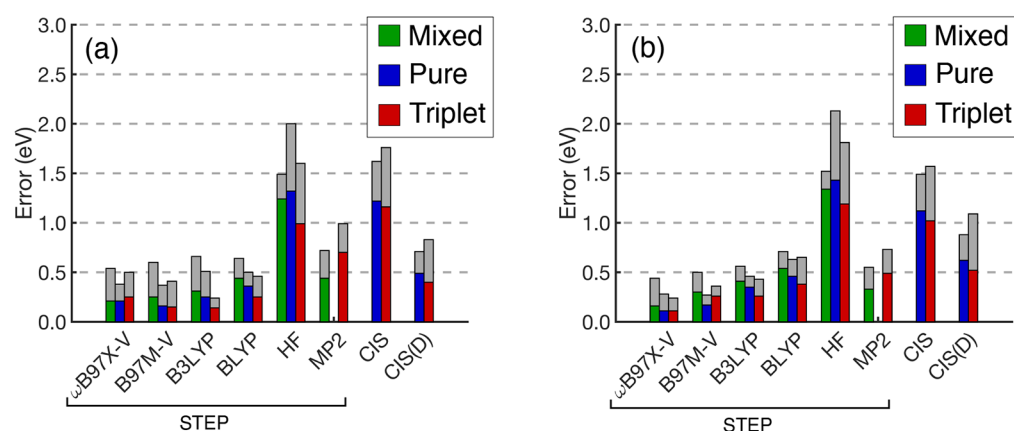


Figure 4. Errors in H_2CO excitation energies with respect to (a) experimental benchmarks from ref 144 or (b) theoretical best estimates from ref 146. Gray bars indicate maximum errors, and colored bars indicate mean absolute errors, color-coded by spin. The aug-cc-pVTZ basis set is used for the STEP calculations, and for singlet excitations we compare both spin-mixed results and spin-purified results; see eq 8. On the far right in both panels are results from the traditional CIS and CIS(D) methods, computed using the 6-311(2+,2+)G(d,p) basis set and taken from ref 1.

Table 1. Excitation Energies (in eV) for Doubly-Excited States

molecule	transition	STEP-DFT ^a			
		$\omega\text{B97X-V}$	B97M-V	CC3 ^b	TBE ^c
Be	$2s^2 \rightarrow 2p^2$	7.55	7.13	7.08	7.06
formaldehyde	$n^2 \rightarrow (\pi^*)^2$	10.20	10.09	11.18	10.34
nitroxy	$n^2 \rightarrow (\pi^*)^2$	4.32	4.41	5.21	4.32
ethylene	$\pi^2 \rightarrow (\pi^*)^2$	12.80	12.48	12.80	12.56
glyoxal	$n^2 \rightarrow (\pi^*)^2$	6.63	5.65	6.76	5.54
pyrazine	$n^2 \rightarrow (\pi^*)^2$	9.07	8.14	9.17	8.04
tetrazine	$^1A_g(n^2 \rightarrow (\pi^*)^2)$	5.65	4.82	6.18	4.60
tetrazine	$^3B_{3g}(n^2 \rightarrow \pi_1^* \pi_2^*)$	6.58	5.52	7.34	5.51
tetrazine	$^1B_{3g}(n^2 \rightarrow \pi_1^* \pi_2^*)$	6.55	5.68	7.60	6.14
MAD ^d		0.61	0.15	0.97	
Max ^e		1.09	0.46	1.83	

^adef2-TZVPPD basis set. ^bExtrapolated to the complete-basis limit, from ref 145. ^cTheoretical best estimates, from ref 145. ^dMean absolute deviation with respect to TBE values. ^eMaximum deviation with respect to TBE values.

will evaluate both DFT-based ΔSCF excitation energies, using several different density functionals, as well as ΔMP2 results in which the correlation is computed using a non-Aufbau reference determinant formed from HF orbitals, optimized using the STEP algorithm.

Figure 4 summarizes the statistical accuracy of various STEP-based approaches across these 11 excited states. Error statistics are computed separately using experimental data as the benchmarks (Figure 4a)¹⁴⁴ versus using theoretical best estimate (TBE) values as benchmarks (Figure 4b).¹⁴⁶ The calculated excitation energies themselves can be found in Table S1. Note that the choice of the best experimental excitation energies for comparison is unclear, with estimates for the $n \rightarrow \pi^*$ excitation ranging from 3.9–4.1 eV.¹⁴⁶ Despite this ambiguity, STEP-SCF results with four different density functionals generally compare well to experiment.

The TBE benchmarks are less ambiguous and are estimated to be within ± 0.03 eV of exact vertical transition energies.¹⁴⁶ In comparison to TBE values, STEP-DFT results using the $\omega\text{B97X-V}$ functional¹⁴⁷ afford the best results among the functionals considered here. The quality of the four sets of STEP-DFT results, as compared to TBE values, is roughly consistent with the Jacob's ladder paradigm,¹⁴⁸ with errors in the order

$$\omega\text{B97X-V} < \text{B97M-V} \lesssim \text{B3LYP} < \text{BLYP}$$

for the functionals $\omega\text{B97X-V}$ (rung 4),¹⁴⁷ B97M-V (rung 3),¹⁴⁹ B3LYP (rung 4),^{150,151} and BLYP (rung 2).^{151,152} Unsurprisingly, errors obtained from HF theory are much larger, regardless of which set of benchmarks is used for comparison. Addition of post-HF correlation dramatically improves the results, and ΔMP2 errors are similar to (if slightly larger than) ΔDFT results. With respect to TBE values, overall errors obtained using STEP-based ΔMP2 calculations are slightly smaller than CIS(D) errors, which is interesting given that the latter method is the excited-state analogue of MP2.¹⁵³

For singlet excited states, note that Figure 4 presents ΔSCF error statistics both with and without spin purification of the type described in Section II.D. For the DFT functionals, spin purification reduces the errors across the board. (Purification slightly increases the already large ΔHF errors, but we do not ascribe much significance to this result owing to the lack of electron correlation.) On average, singlet excitation energies predicted via spin-purified ΔDFT improve by about 0.05 eV as compared to their spin-mixed counterparts, with the largest correction being 0.1 eV. The smallness of this correction was predictable in view of the rather similar error statistics obtained for singlet versus triplet excitation energies. However, the small magnitude of the energy correction in eq 8 does not indicate that

Table 2. Excitation Spectrum of H₂O (in eV) Computed Using STEP-Based Methods

transition	HF ^{a,b}	MP2 ^{b,c}	spin-biased MP2 ^{b,c}			DFT ^{a,d}		benchmarks	
			SCS	SOS	MOS ^e	B97M-V	ω B97X-V	expt ^f	TBE ^g
¹ B ₁ (<i>n</i> → 3s)	6.29 (6.51)	7.83	7.78	7.75	7.59	7.47 (7.75)	7.58 (7.75)	7.41	7.70
¹ A ₂ (<i>n</i> → 3p)	8.07 (8.16)	9.73	9.66	9.62	9.46	9.11 (9.23)	9.47 (9.57)	9.20	9.47
¹ A ₁ (<i>n</i> → 3s)	8.83 (9.23)	10.16	10.14	10.12	9.96	9.82 (10.15)	9.91 (10.15)	9.67	9.97
³ B ₁ (<i>n</i> → 3s)	6.07	7.62	7.60	7.59	7.42	7.19	7.41	7.20	7.33
³ A ₂ (<i>n</i> → 3p)	7.97	9.64	9.58	9.55	9.39	9.00	9.37	8.90	9.30
³ A ₁ (<i>n</i> → 3s)	8.43	9.91	9.90	9.89	9.73	9.49	9.66	9.46	9.59
MAD (expt)	1.03 (0.91)	0.51	0.47	0.45	0.29	0.07 (0.17)	0.26 (0.35)		0.25
MAD (TBE)	1.28 (1.17)	0.25	0.22	0.19	0.08	0.21 (0.17)	0.07 (0.10)		

^aSpin-purified results for singlets (eq 8) are given in parentheses. The corresponding MAD includes the triplets. ^bdef2-QZVPPD basis set. ^cFrozen core. ^ddef2-TZVPPD basis set. ^eUsing a range-separation parameter $\omega = 0.6$ bohr⁻¹. ^fExperimental data from ref 158. ^gTheoretical best estimates, from ref 146.

the spin contamination itself is small, as $\langle \hat{S}^2 \rangle \approx 1.01$ (in atomic units) for all of the singlet excited states of H₂CO. For the ¹B_{1u} state of C₂H₄, where an error of 1.8 eV is reduced to 0.3 eV upon spin purification [B3LYP/6-311(2+,2+)G** level],¹ we find that $\langle \hat{S}^2 \rangle = 1.00$. Unfortunately, this suggests that the value of $\langle \hat{S}^2 \rangle$ is not a useful diagnostic for whether the energy correction upon spin purification will be large or not, although we find that even the spin-contaminated results for H₂CO are rather accurate.

Overall, affordable STEP-based methods compare very well to high-accuracy benchmarks for H₂CO, and the performance of STEP-based Δ MP2 is promising for situations where one might wish to avoid DFT. Interestingly, spin-contaminated HF wave functions appear to be sufficient for Δ MP2 to outperform CIS(D) with respect to theoretical benchmarks.

III.C. Double Excitations. STEP-DFT results for these benchmarks are presented in Table 1, and SGM-DFT results for the same data set can be found in ref 119. Consistent with that study, we find that the ω B97X-V functional performs significantly worse than B97M-V for these benchmarks. The performance of B97M-V is quite good (maximum error <0.5 eV) given the difficult nature of the problem. Orbital relaxation effects are generally larger for double excitations, as the doubly excited character represents a complete breakdown of the ground-state orbitals in describing the excited state, and even the CC3 method affords errors for these benchmarks that are significantly larger than those obtained using STEP-DFT.

III.D. Non-Aufbau States of H₂O. Excited states of H₂O in the gas phase are Rydberg in nature, having nearly pure single-excitation character that should be readily amenable to single-determinant methods like STEP, but which are quite challenging for TD-DFT.^{154–157} Both experimental values¹⁵⁸ and highly accurate TBE benchmarks¹⁴⁶ are available, although the latter likely make for a cleaner comparison because the fitting of the experimental spectrum (from which the “vertical” excitation energies are extracted) is not straightforward.¹⁵⁸ Excitation energies for the lowest six excited states, obtained using STEP at different levels of theory, are presented in Table 2.

The ω B97X-V and B97M-V functionals are tested due to their excellent performance for H₂CO, and both perform quite well for H₂O also. Interestingly, it is not clear that spin purification is beneficial in this case, as it generally has only a very small effect on the energy and leads to a very slight increase in the average error in the case of ω B97X-V.

Results using MP2, along with several spin-scaled variants thereof, offer interesting insight into the description of Rydberg

excitations. All MP2 calculations were performed using the def2-QZVPPD basis set^{159,160} in order to reduce basis incompleteness effects. As expected, STEP-based Δ MP2 (using the conventional MP2 method) significantly improves upon the performance of STEP-based Δ HF, the latter of which exhibits errors of ~ 1 eV, roughly the correlation energy per pair of electrons. This perhaps suggests that the excitation can be roughly divided into orbital relaxation effects, which are described at the STEP-HF level, and electron correlation effects that are not. Incorporating correlation at the MP2 level on top of the STEP-HF determinant reduces the mean absolute deviation (MAD) to 0.25 eV with respect to TBE values.

Also examined in Table 2 are several “spin-biased” versions of MP2, including spin-component scaled (SCS),¹⁶¹ scaled opposite-spin (SOS),¹⁶² and modified opposite-spin (MOS) variants.¹⁶³ The results afford interesting insights into the limitations of second-order perturbation theory and how best to address these limitations in the context of a reference determinant optimized using STEP-HF. For the excited states of H₂O, the SCS- and SOS-MP2 variants afford very similar excitation energies that are only marginal improvements upon the canonical STEP-MP2 results. However, MOS-MP2 performs quite a bit better with a mean error of <0.1 eV. This difference can be understood based on the asymptotic behavior of the correlation energy in each case. Each of these spin-biased MP2 methods corresponds to an *ansatz* for the correlation energy of the form

$$E_{\text{corr}} = c_{\text{ss}}E_{\text{corr,ss}} + c_{\text{os}}E_{\text{corr,os}} \quad (9)$$

where c_{ss} and c_{os} are scaling factors for the same- and opposite-spin components of the conventional MP2 correlation energy. For a closed-shell system, consideration of the correlation energy between well-separated fragments suggests a constraint $c_{\text{os}} + c_{\text{ss}} = 2$,¹⁶³ which the scaling factors used in practice do not satisfy. (The parameters used for SCS-MP2 are $c_{\text{os}} = 1.2$ and $c_{\text{ss}} = 0.3$,¹⁶¹ versus $c_{\text{os}} = 1.3$ and $c_{\text{ss}} = 0$ for SOS-MP2.¹⁶²) Both pairs of coefficients lead to a systematic underestimation of long-range correlation, and of course asymptotic behavior is key to a proper description of Rydberg states. The MOS-MP2 approach maintains the correct asymptotic behavior of the correlation energy by means of range separation¹⁶³ and is therefore much more suitable for use in the description of Rydberg excitations.

Application of STEP to converge non-Aufbau states is not limited to electronically excited states; ionized valence- and core-hole states can be obtained as well. This is important given that valence photoelectron spectroscopy beyond the first

Table 3. Vertical Ionization Energies for H₂O (in eV) Computed Using STEP-Based Methods

orbital	HF ^a	MP2 ^{a,b}	spin-biased MP2 ^{a,b}			DFT ^c		expt
			SCS	SOS	MOS ^d	B97M-V	ω B97X-V	
1b ₁	10.97	12.95	12.85	12.80	12.66	12.64	12.71	12.61 ^e
3a ₁	13.24	15.14	15.06	15.02	14.89	14.87	14.87	14.84 ^f
1b ₂	17.43	19.27	19.19	19.15	19.02	18.98	18.91	18.78 ^f
2a ₁	34.06	34.00	33.80	33.70	33.64	33.47	32.68	32.62 ^f
MAD	1.51	0.63	0.51	0.46	0.34	0.28	0.08	
Max	1.64	1.38	1.18	1.08	1.02	0.85	0.13	

^aaug-cc-pCVQZ basis set. ^bCorrelating all electrons. ^caug-cc-pCVTZ basis set. ^dUsing range-separation parameter $\omega = 0.6$ bohr⁻¹. ^eReference 168. ^fReference 169.

ionization energy remains a challenge for theory.^{103,164} Note also that X-ray absorption spectra computed with TD-DFT often exhibit large errors,^{107,165–167} owing to a combination of self-interaction error and problems with the description of long-range charge transfer, so core-level excitation spectra are also interesting targets for methods such as STEP. Here, however, we limit the discussion to ionized states of H₂O.

Table 3 presents the full valence photoelectron spectrum of H₂O computed using STEP-based Δ SCF and Δ MP2 methods. Mean errors for the MP2 variants are generally comparable to the errors obtained for excitation energies of the same molecule, especially if the “semi-core” $(2a_1)^{-1}$ state is excluded, which affords the largest error for each of the MP2 variants. Among these MP2 methods, the improvement gained from the asymptotically correct behavior of MOS-MP2 is notably less significant here than it was for the valence excitations in Table 2, and errors for both SCS- and SOS-MP2 are about the same. This is likely due to the fact the wave function for the final (cationic) state is relatively compact and therefore does not sample the asymptotic part of the Coulomb potential, making ionization energies much less sensitive to asymptotics as compared to Rydberg excitation energies. In an effort to obtain a good description of the $(2a_1)^{-1}$ state, the MP2 calculations in Table 3 employ a basis set that includes core/valence polarization functions (aug-cc-pCVQZ),^{170,171} and core electrons are included in the MP2 correlation energy for these calculations; nevertheless, errors of ≈ 1 eV persist in the $(2a_1)^{-1}$ ionization energy at MP2-based levels of theory.

The Δ DFT results are quite a bit better than the Δ MP2 results, especially for the $(2a_1)^{-1}$ state. The ω B97X-V functional shows an outstanding performance (MAD < 0.1 eV), while B97M-V exhibits slightly larger errors (MAD = 0.3 eV) but still outperforms each of the MP2 variants. These results are consistent with those obtained using SGM-based restricted open-shell Kohn–Sham (ROKS) calculations.¹⁷² We conclude that the STEP-based Δ DFT approach to computing full excitation spectra seems quite promising and warrants a more complete investigation in subsequent work.

E. X-ray Photoelectron Spectroscopy. Core-level photoelectron spectroscopy is an important analytical technique in chemistry and materials science,^{173,174} and Δ SCF procedures are common in modeling core-ionized states.^{100–105} Self-interaction error is considerably larger in core as compared to valence energy levels, due to the relative compactness of the orbitals in question, and this error generally decreases with increasing fraction of exact exchange.⁹ It is therefore surprising that comprehensive assessments of Δ DFT for core–electron binding energies (CEBEs) do not indicate that hybrid functionals are systematically more accurate as compared to semilocal functionals.^{100,101,175}

As discussed in Section II.C, the efficiency of STEP is expected to decrease as the magnitude of the level shift increases. Creating a core hole requires a level shift of several hundred eV or more, and indeed we find that this negatively impacts the efficiency of STEP-SCF calculations. Nevertheless, we are able to optimize core-ionized states, and in Table 4 we compare CEBEs, computed with Δ SCF calculations, to experiment. All calculations were performed using the cc-pCVTZ basis set with the SCF convergence threshold set to 10^{-8} Ha.

Table 4. Δ SCF Binding Energies for 1s Electrons (in eV)^a

molecule ^b	HF	B3LYP	B97M-V	ω B97X-V	expt
H ₂ O	538.90	539.47	541.23	539.72	539.82 ^c
CO ₂	299.13	297.84	298.98	298.15	297.69 ^d
NH ₃	405.06	405.34	406.95	405.60	405.56 ^d
H ₃ CCN	404.92	405.34	406.86	405.64	405.64 ^d
HF	692.89	693.36	695.25	693.54	694.23 ^d
HCHO	537.96	538.85	540.66	539.05	539.48 ^d
CH ₄	290.57	290.85	292.22	291.04	290.91 ^d
NNO	408.39	408.56	410.05	408.84	408.71 ^d
NNO	413.74	412.56	413.97	413.02	412.59 ^d
NNO	540.33 ^e	541.19	543.03	541.33	541.42 ^d
CO	296.40	296.59	297.85	296.80	296.21 ^d
CO	541.30	542.09	543.79	542.29	542.55 ^d
MAD ^f	0.90	0.32	1.34	0.28	
MSD ^g	−0.44	−0.23	1.34	0.02	
Max ^h	1.44	0.38	1.64	0.59	

^aSTEP ($e' = 1$ Ha) and IMOM results are equivalent unless indicated otherwise. ^bCalculations correspond to the $(1s)^{-1}$ state of the indicated atom. ^cReference 176. ^dReference 177. ^eMOM and IMOM calculations do not converge to 10^{-8} Ha. ^fMean absolute deviation with respect to experiment. ^gMean signed deviation. ^hMaximum error.

We find that ω B97X-V exhibits excellent performance for these benchmarks and significantly smaller errors as compared to B97M-V. Indeed, errors obtained using B97M-V are even larger than those afforded by HF theory and with a systematic bias toward overestimation of the CEBE, whereas HF theory systematically underestimates CEBEs. The MAD obtained using B3LYP is similar to the value obtained with ω B97X-V; however, B3LYP systematically underestimates CEBEs, whereas the mean signed deviation for ω B97X-V is close to zero, indicating the absence of systematic error.

Although the STEP approach is less efficient for optimizing a core hole as compared to a valence hole, it remains a robust alternative to MOM and IMOM. In the case of the O(1s) ionization of N₂O, both overlap-based algorithms achieve a loose convergence threshold of 10^{-5} Ha but then become oscillatory, whereas the RMS error for the STEP-SCF procedure

decreases monotonically until the desired precision is reached (see Figure S2). Using the loosely converged MOM solution changes the CEBE by only 0.2 eV, which is small relative to the absolute value in question (541 eV), but on the other hand, the quality of the SCF wave function can have an impact on property calculations or post-HF correlation calculations. As such, it is desirable to be able to achieve tight convergence. As compared to MOM-SCF, the STEP-SCF procedure is a slower but reliable procedure for computing CEBEs.

F. Vertical and Adiabatic Ionization of 2,4,6-Trifluoroborazine. In the applications above, we have considered vertical ionization of both core and valence electrons, but in some cases, adiabatic ionization energies may be of interest. Calculation of these quantities requires geometry optimization in the presence of a core or valence hole. This poses a challenge for theoretical methods in that a consistent electronic state must be maintained throughout the course of a geometry optimization of the ionized final state. Fortunately, the STEP algorithm is merely a trick to maintain the desired occupancies throughout optimization of the density and does not alter the nuclear gradients, so only ground-state analytic gradient technology is required. Here, we benchmark the performance of STEP against experimental data for the vertical and adiabatic ionization energies of the molecule 2,4,6-trifluoroborazine. Results using both STEP and IMOM are presented in Table 5, using the ω B97X-V functional.

Table 5. Ionization Energies (in eV) of 2,4,6-Trifluoroborazine^a

orbital	vertical			adiabatic		
	ω B97X-V	expt ^b	error	ω B97X-V	expt ^b	error
4b ₂	10.84	10.79	0.05	10.42	10.46	0.04
3b ₂	12.94	12.98	0.04	12.78	12.85	0.07
11b ₁	13.42	13.53	0.11	12.85	13.35	0.50
10b ₁	14.07	14.29	0.22	13.79	14.05	0.26
2b ₂	15.92	15.85	0.07	15.39	15.42	0.03
1b ₂ ^c	16.23	16.20	0.03	16.10	16.11	0.01
8b ₁	16.61	16.87	0.26	16.31	16.69	0.38
13a ₁	17.94	17.73	0.21	17.70	17.67	0.03
MAD			0.12			0.16
Max			0.26			0.50

^aSTEP and IMOM results are equivalent unless indicated otherwise.

^bReference 178. ^cIMOM calculation of the adiabatic ionization energy did not converge.

Errors obtained using ω B97X-V are slightly larger as compared to the case of vertical ionization energies of H₂O, but the MADs versus experiment for vertical ionization (0.1 eV) and adiabatic ionization (0.2 eV) are still quite reasonable. For nearly every ionized state, we obtain precisely the same final-state energies using both STEP and IMOM, with the lone exception being adiabatic ionization of the (1b₂)⁻¹ state. In that case, the IMOM algorithm oscillates and fails to converge after more than 600 SCF cycles. In contrast, we encounter no problems in optimizing the proper states using STEP-DFT.

G. Chlorophyll *a*: Isolating Key Excitations. In our final application we consider the photoactive Mg-chlorin ring of chlorophyll *a* (Chl *a*). Chloroplasts (the organelles in plants that conduct photosynthesis) contain mixtures of Chl *a* and Chl *b*, which act as the light-harvesting centers for photosynthesis, and Chl *a* is a primary electron donor in the electron transport chain. Its absorption spectrum is largely comprised of red/orange and

blue/violet light, reflecting the green/yellow parts of the spectrum that are responsible for the color of most plants. The excitations responsible for the absorption spectrum are mostly contained in the first few $\pi \rightarrow \pi^*$ transitions and are understood in terms of Gouterman's four-orbital model.¹⁷⁹ The low-energy (red/orange) band in the spectrum is commonly called the "Q-band", and the higher-energy (blue/violet) features are known as the "Soret band".

Most studies of Chl *a* have been conducted in a solvent (e.g., methanol or diethyl ether); however, gas-phase absorption spectra for both the Q-band and the Soret band have been reported recently.^{180,181} This makes for a more straightforward comparison with *ab initio* calculations. In biological systems, the photoactive chlorin of Chl *a* is attached to a long hydrocarbon tail that anchors Chl *a* to the cell membrane, but this tail is a spectator with regard to the photophysics and is not necessary to retain the critical spectral properties of the system.¹⁸² We have applied STEP to the photoactive region of a truncated model of gas-phase Chl *a*, obtaining spin-purified singlet excitation energies that are superimposed with the experimental spectrum in Figure 5a.

Qualitatively, the STEP-based Δ SCF excitation spectrum (based on the four-orbital model) captures the appropriate spectral range of light that would be absorbed by Chl *a*, predicting peaks in the orange, red, violet, and ultraviolet (UV) parts of the spectrum with no excitations in green/yellow

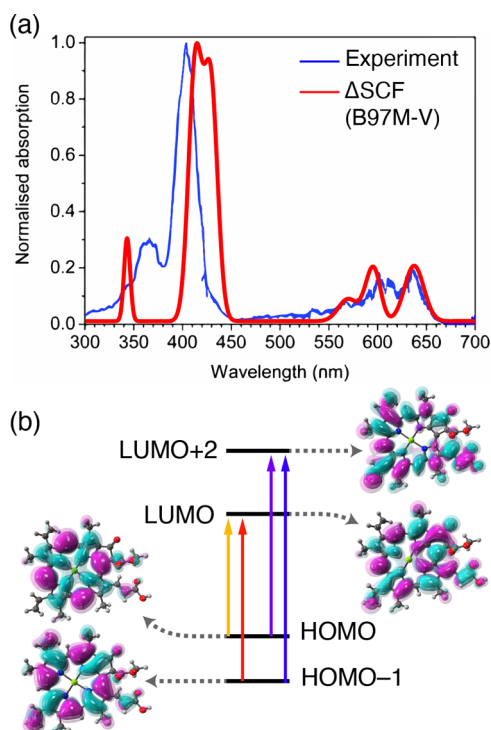


Figure 5. (a) Absorption spectrum of Chl *a* computed using STEP-based Δ DFT at the B97M-V/def2-TZVP level of theory and superimposed on the experimental spectrum from ref 180. The vertical excitation spectrum obtained from the calculations has been broadened using a Gaussian line shape and normalized to match the experimental absorption maximum. (b) Four-orbital model (at the same level of theory) that recovers the major features of the Chl *a* spectrum. The computed spectrum in (a) is constructed from Δ SCF calculations of the four transitions that are indicated in (b). Excitation energies have been purified using eq 8. The experimental spectrum is reproduced from ref 180. Copyright 2015 the PCCP Owner Societies.

regions. The Q-band maximum in gas-phase Chl *a* was measured at 1.9 eV (642 nm), and the first two Δ SCF excitation energies deviate from the experimental band maximum by only 0.01–0.10 eV (i.e., only by 2–40 nm). The second two excitation energies appear to capture the higher-energy shoulder of the Q-band, centered around 2.1 eV (590 nm). In the high-energy regime, the Δ SCF calculation correctly captures not only the Soret band but also the higher-energy UV shoulder. The two excitations that can be assigned as Soret-band peaks differ from the experimental band maximum of 3.1 eV (405 nm) by 0.1–0.2 eV (11–30 nm). Finally, the UV shoulder of the Soret band is centered at 3.4 eV (365 nm) in the experimental spectrum, and the Δ SCF results are within 0.2 eV (22 nm) of experiment.

The fact that the spectrum emerges so cleanly from these Δ SCF calculations can be considered an affirmation of Gouterman's model (Figure 5b). The Q-band is attributed to HOMO \rightarrow LUMO and (HOMO $-$ 1) \rightarrow LUMO excitations, whereas the Soret-band peaks emerge from HOMO \rightarrow (LUMO + 2) and (HOMO $-$ 1) \rightarrow (LUMO + 2) excitations. The shoulder on the high-energy Soret band consists of excitations out of the HOMO and HOMO $-$ 1 and into LUMO + 3, but this shoulder is not considered in Gouterman's model. Using STEP, we have recovered a simple four-orbital representation for the key excitations involved in the absorption spectrum of Chl *a*.

That said, one might question whether a single-determinant approximation to the excited-state wave functions is appropriate for a system with quasi-degenerate frontier orbitals. It is therefore worth noting that Gill and co-workers have applied IMOM to study C_6H_6 ,⁴ where both the HOMO ($1e_{1g}$) and LUMO ($1e_{2u}$) are doubly degenerate. The $^1E_{2g}$ excited state of C_6H_6 is traditionally understood to involve a significant contribution from a (HOMO)² \rightarrow (LUMO)² double excitation,^{183,184} nevertheless, the Δ SCF excitation energy for this state, computed at the BLYP/6-311G* level, is accurate to within 0.1 eV.⁴ The "excitation number" for the $^1E_{2g}$ state,⁸³ which measures the number of electrons that are promoted, based on overlap of the initial- and final-state occupied MOs, is only 1.0058.⁴ As such, an alternative description of the $^1E_{2g}$ state is that it involves a significant change in the density, which is associated with significant orbital relaxation, but double excitations need not be invoked (in a qualitative description) if the excited-state wave function is allowed to use different MOs as compared to the ones optimized for the ground state. Within the more traditional picture, multideterminantal character is needed to compensate for the constraint that the orbital basis is not allowed to change.

In addition to B97M-V, we have also computed the Chl *a* spectrum using the ω B97X-V and SCAN¹⁸⁵ functionals; see Table 6. The performance of ω B97X-V is quite poor, with errors exceeding 1 eV. In light of the comments above regarding quasi-degenerate orbitals, and thus the likely multideterminantal nature of the low-lying excited states in Chl *a*, it is noteworthy that ω B97X-V also performs poorly for double-excitation benchmarks (Section III.C). This suggests that ω B97X-V may perform poorly, in general, in cases where the excited state has significant multideterminant character. In contrast, Δ SCF results obtained from the SCAN functional are nearly as accurate as those obtained using B97M-V, and it is again noteworthy that these were the two best-performing functionals for double-excitation benchmarks computed using SGM.¹¹⁹ These functionals may be particularly well-suited to describe states with multideterminant character

Table 6. Spin-Purified Excitation Energies (in eV) for Chl *a*

transition	STEP-based Δ SCF			expt
	ω B97X-V	B97M-V	SCAN	
HOMO \rightarrow LUMO	3.07	2.06	1.99	1.93 (Q) ^a
HOMO $-$ 1 \rightarrow LUMO	3.28	1.93	1.78	
HOMO \rightarrow LUMO + 1	3.35	2.17	1.99	
HOMO $-$ 1 \rightarrow LUMO + 1	3.37	2.08	1.87	
HOMO \rightarrow LUMO + 2	4.29	2.98	2.88	3.06 (S) ^b
HOMO $-$ 1 \rightarrow LUMO + 2	4.28	2.87	2.66	
HOMO \rightarrow LUMO + 3	4.59	3.61	3.34	3.40 (SS) ^c
HOMO $-$ 1 \rightarrow LUMO + 3	4.38	3.61	3.38	

^aQ-band ("Q"), from ref 181. ^bSoret band ("S"), from ref 180. ^cSoret band shoulder ("SS"), from ref 180.

Previous TD-DFT calculations of Chl *a* required 15 excited states, many of which with near-zero oscillator strengths, in order to resolve the Soret band.¹⁸⁰ Some or all of these may be spurious low-energy charge-transfer states,²⁵ which can plague large-molecule TD-DFT calculations,²⁴ although calculations in ref 180 were performed with the range-separated CAM-B3LYP hybrid functional.¹⁸⁶ In any case, it is encouraging that the gross features of the absorption spectrum (i.e., the bright states) can be recovered in a very simple fashion using STEP.

IV. CONCLUSIONS

We have introduced a novel algorithm ("STEP") for converging non-Aufbau solutions to the SCF equations. It is intended as an alternative to overlap-based procedures such as MOM¹ and IMOM,⁴ and also as an alternative to the recently introduced SGM method.¹¹⁹ STEP appears to be more robust than MOM or IMOM and is more efficient than SGM. Like MOM (but unlike SGM), the STEP algorithm requires only a single Fock build per iteration. Although its reliability is only as good as the initial guess configuration, we find that SGM can also suffer from sensitivity to the initial guess, as noted elsewhere.¹¹⁹

In principle, STEP is guaranteed to converge to the nearest stationary point in the space of MO coefficients. Although SGM has something of an advantage in that it can escape cases of an initial guess in the "wrong" MO configuration, we have shown that STEP can optimize very difficult non-Aufbau configurations when SGM collapses to a nearby stationary point that is qualitatively different from the target state of interest. Meanwhile, STEP is generally more reliable than MOM or IMOM, because it guarantees that the initial configuration is carried through to the end of the optimization. Unlike MOM or IMOM, which can suddenly (and discontinuously) switch electron configurations in cases where the overlap criterion becomes ambiguous, sometimes leading to variational collapse, the STEP algorithm has no choice but to deform the MOs in a continuous manner starting from the user-specified initial set. Overall, STEP appears to be an exceptionally robust alternative to overlap-based procedures, rivaling the reliability of SGM but without the increased cost.

In addition to numerous benchmark tests, we have considered a variety of chemically interesting applications as well. Analysis of Rydberg excitations provides insight into the importance of the long-range behavior of the correlation energy in spin-biased MP2 methods (including SCS-, SOS-, and MOS-MP2). Excellent accuracy for both core- and valence ionization energies is documented. Furthermore, the STEP algorithm is robust enough to be used for geometry optimization of both valence- and core-hole states, so that adiabatic ionization energies can be

computed in addition to vertical ionization energies. Valence excitation energies of a large chemical system (Chl *a*), and of challenging test cases involving states with double-excitation character, have been computed with at least semiquantitative accuracy.

Prospects for the STEP algorithm seem most exciting in condensed-phase applications, which are computationally expensive, and therefore SGM is a comparatively less appealing option. Furthermore, conduction-band states are fraught with numerous near-degeneracies that can easily cause variational collapse in overlap-based algorithms. Nuclear gradients are unchanged by the STEP procedure, which opens a pathway for performing excited-state (non-Aufbau) dynamics at mean-field cost.

■ ASSOCIATED CONTENT

SI Supporting Information

The Supporting Information is available free of charge at <https://pubs.acs.org/doi/10.1021/acs.jctc.0c00502>.

Additional data on performance of STEP (PDF)
xyz file (XYZ)

■ AUTHOR INFORMATION

Corresponding Authors

Kevin Carter-Fenk – Department of Chemistry and Biochemistry, The Ohio State University, Columbus, Ohio 43210, United States; orcid.org/0000-0001-8302-4750; Email: carter-fenk.2@osu.edu

John M. Herbert – Department of Chemistry and Biochemistry, The Ohio State University, Columbus, Ohio 43210, United States; orcid.org/0000-0002-1663-2278; Email: herbert@chemistry.ohio-state.edu

Complete contact information is available at: <https://pubs.acs.org/doi/10.1021/acs.jctc.0c00502>

Notes

The authors declare the following competing financial interest(s): J.M.H. serves on the board of directors of Q-Chem Inc.

■ ACKNOWLEDGMENTS

This work was supported by the U.S. Department of Energy, Office of Basic Energy Sciences, Division of Chemical Sciences, Geosciences, and Biosciences under Award No. DE-SC0008550. Calculations were performed at the Ohio Supercomputer Center under project no. PAA-0003.¹⁸⁷ K.C.-F. acknowledges a Presidential Fellowship from The Ohio State University.

■ REFERENCES

- (1) Gilbert, A. T. B.; Besley, N. A.; Gill, P. M. W. Self-consistent field calculations of excited states using the maximum overlap method (MOM). *J. Phys. Chem. A* **2008**, *112*, 13164–13171.
- (2) Deng, J.; Gilbert, A. T. B.; Gill, P. M. W. Rydberg states of the helium atom. *Int. J. Quantum Chem.* **2009**, *109*, 1915–1919.
- (3) Barca, G. M. J.; Gilbert, A. T. B.; Gill, P. M. W. Communication: Hartree-Fock description of excited states of H₂. *J. Chem. Phys.* **2014**, *141*, 111104.
- (4) Barca, G. M. J.; Gilbert, A. T. B.; Gill, P. M. W. Simple models for difficult electronic excitations. *J. Chem. Theory Comput.* **2018**, *14*, 1501–1509.

- (5) Del Bene, J. E.; Ditchfield, R.; Pople, J. A. Self-consistent molecular orbital methods. X. Molecular orbital studies of excited states with minimal and extended basis sets. *J. Chem. Phys.* **1971**, *55*, 2236–2241.

- (6) Foresman, J. B.; Head-Gordon, M.; Pople, J. A.; Frisch, M. J. Toward a systematic molecular orbital theory for excited states. *J. Phys. Chem.* **1992**, *96*, 135–149.

- (7) Dreuw, A.; Head-Gordon, M. Single-reference ab initio methods for the calculation of excited states of large molecules. *Chem. Rev.* **2005**, *105*, 4009–4037.

- (8) Casida, M. E. Time-dependent density functional response theory for molecules. In *Recent Advances in Density Functional Methods, Part I*; Chong, D. P., Ed.; World Scientific: River Edge, NJ, 1995; Vol. I, 155–192, .

- (9) Petersilka, M.; Gossmann, U. J.; Gross, E. K. U. Excitation energies from time-dependent density-functional theory. *Phys. Rev. Lett.* **1996**, *76*, 1212–1215.

- (10) Bauernschmitt, R.; Ahlrichs, R. Treatment of electronic excitations within the adiabatic approximation of time dependent density functional theory. *Chem. Phys. Lett.* **1996**, *256*, 454–464.

- (11) Stratmann, R. E.; Scuseria, G. E.; Frisch, M. J. An efficient implementation of time-dependent density-functional theory for the calculation of excitation energies of large molecules. *J. Chem. Phys.* **1998**, *109*, 8218–8224.

- (12) Furche, F. On the density matrix based approach to time-dependent density functional response theory. *J. Chem. Phys.* **2001**, *114*, 5982–5992.

- (13) Furche, F.; Ahlrichs, R. Adiabatic time-dependent density functional methods for excited state properties. *J. Chem. Phys.* **2002**, *117*, 7433–7447; Erratum: **2004**, *121*, 12772–12773.

- (14) Furche, F.; Rappoport, D. Density functional methods for excited states: Equilibrium structure and electronic spectra. In *Computational Photochemistry*; Olivucci, M., Ed.; Elsevier: Amsterdam, 2005; Vol. 16, 93–128, .

- (15) Rappoport, D.; Furche, F. Analytical time-dependent density functional derivative methods within the RI-J approximation, an approach to excited states of large molecules. *J. Chem. Phys.* **2005**, *122*, 064105.

- (16) Hanson-Heine, M. W. D.; George, M. W.; Besley, N. A. Assessment of time-dependent density functional theory calculations with the restricted space approximation for excited state calculations of large systems. *Mol. Phys.* **2018**, *116*, 1452–1459.

- (17) Laurent, A. D.; Jacquemin, D. TD-DFT benchmarks: A review. *Int. J. Quantum Chem.* **2013**, *113*, 2019–2039.

- (18) Casida, M. E.; Gutierrez, F.; Guan, J.; Gadea, F.-X.; Salahub, D.; Daudey, J.-P. Charge-transfer correction for improved time-dependent local density approximation excited-state potential energy curves: Analysis within the two-level model with illustration for H₂ and LiH. *J. Chem. Phys.* **2000**, *113*, 7062–7071.

- (19) Dreuw, A.; Weisman, J. L.; Head-Gordon, M. Long-range charge-transfer excited states in time-dependent density functional theory require non-local exchange. *J. Chem. Phys.* **2003**, *119*, 2943–2946.

- (20) Dreuw, A.; Head-Gordon, M. Failure of time-dependent density functional theory for long-range charge-transfer excited-states: The zincbacteriochlorin–bacteriochlorin and bacteriochlorophyll–spheroidene complexes. *J. Am. Chem. Soc.* **2004**, *126*, 4007–4016.

- (21) Bernasconi, L.; Sprik, M.; Hutter, J. Hartree-Fock exchange in time dependent density functional theory: Application to charge transfer excitations in solvated molecular systems. *Chem. Phys. Lett.* **2004**, *394*, 141–146.

- (22) Neugebauer, J.; Louwse, M. J.; Baerends, E. J.; Wesolowski, T. A. The merits of the frozen-density embedding scheme to model solvatochromatic shifts. *J. Chem. Phys.* **2005**, *122*, 094115.

- (23) Neugebauer, J.; Gritsenko, O.; Baerends, E. J. Assessment of a simple correction for the long-range charge-transfer problem in time-dependent density functional theory. *J. Chem. Phys.* **2006**, *124*, 214102.

- (24) Magyar, R. J.; Tretiak, S. Dependence of spurious charge-transfer excited states on orbital exchange in TDDFT: Large molecules and clusters. *J. Chem. Theory Comput.* **2007**, *3*, 976–987.

- (25) Lange, A.; Herbert, J. M. Simple methods to reduce charge-transfer contamination in time-dependent density-functional calculations of clusters and liquids. *J. Chem. Theory Comput.* **2007**, *3*, 1680–1690.
- (26) Lange, A. W.; Rohrdanz, M. A.; Herbert, J. M. Charge-transfer excited states in a π -stacked adenine dimer, as predicted using long-range-corrected time-dependent density functional theory. *J. Phys. Chem. B* **2008**, *112*, 6304–6308; Erratum: **2008**, *112*, 7345.
- (27) Peach, M. J. G.; Benfield, P.; Helgaker, T.; Tozer, D. J. Excitation energies in density functional theory: An evaluation and a diagnostic test. *J. Chem. Phys.* **2008**, *128*, 044118.
- (28) Isborn, C. M.; Mar, B. D.; Curchod, B. F. E.; Tavernelli, I.; Martínez, T. J. The charge transfer problem in density functional theory calculations of aqueously solvated molecules. *J. Phys. Chem. B* **2013**, *117*, 12189–12201.
- (29) Levine, B. G.; Ko, C.; Quenneville, J.; Martínez, T. J. Conical intersections and double excitations in time-dependent density functional theory. *Mol. Phys.* **2006**, *104*, 1039–1051.
- (30) Herbert, J. M.; Zhang, X.; Morrison, A. F.; Liu, J. Beyond time-dependent density functional theory using only single excitations: Methods for computational studies of excited states in complex systems. *Acc. Chem. Res.* **2016**, *49*, 931–941.
- (31) Elliott, P.; Goldson, S.; Canahui, C.; Maitra, N. T. Perspective on double-excitations in TDDFT. *Chem. Phys.* **2011**, *391*, 110–119.
- (32) Maitra, N. T. Charge-transfer in time-dependent density functional theory. *J. Phys.: Condens. Matter* **2017**, *29*, 423001.
- (33) Igumenshchev, K. I.; Tretiak, S.; Chernyak, V. Y. Excitonic effects in a time-dependent density functional theory. *J. Chem. Phys.* **2007**, *127*, 114902.
- (34) Mewes, S. A.; Plasser, F.; Dreuw, A. Communication: Exciton analysis in time-dependent density functional theory: How functionals shape excited-state characters. *J. Chem. Phys.* **2015**, *143*, 171101.
- (35) Mewes, S. A.; Plasser, F.; Dreuw, A. Universal exciton size in organic polymers is determined by nonlocal orbital exchange in time-dependent density functional theory. *J. Phys. Chem. Lett.* **2017**, *8*, 1205–1210.
- (36) Subotnik, J. E. Configuration interaction singles has a large systematic bias against charge-transfer states. *J. Chem. Phys.* **2011**, *135*, 071104.
- (37) Liu, X.; Subotnik, J. E. The variationally orbital-adapted configuration interaction singles (VOA-CIS) approach to electronically excited states. *J. Chem. Theory Comput.* **2014**, *10*, 1004–1020.
- (38) Ronca, E.; Angeli, C.; Belpassi, L.; De Angelis, F.; Tarantelli, F.; Pastore, M. Density relaxation in time-dependent density functional theory: Combining relaxed density natural orbitals and multireference perturbation theories for an improved description of excited states. *J. Chem. Theory Comput.* **2014**, *10*, 4014–4024.
- (39) Maschietto, F.; Campetella, M.; Frisch, M. J.; Scalmani, G.; Adamo, C.; Clofini, I. How are the charge transfer descriptors affected by the quality of the underpinning electronic density? *J. Comput. Chem.* **2018**, *39*, 735–742.
- (40) Triguero, L.; Pettersson, L. G. M.; Ågren, H. Calculations of x-ray emission spectra of molecules and surface adsorbates by means of density functional theory. *J. Phys. Chem. A* **1998**, *102*, 10599–10607.
- (41) Leetmaa, M.; Ljungberg, M. P.; Lyubartsev, A.; Nilsson, A.; Pettersson, L. G. M. Theoretical approximations to x-ray absorption spectroscopy of liquid water and ice. *J. Electron Spectrosc. Relat. Phenom.* **2010**, *177*, 135–157.
- (42) Zhang, Y.; Hua, W.; Bennett, K.; Mukamel, S. Nonlinear spectroscopy of core and valence excitations using short x-ray pulses: Simulation challenges. In *Density-Functional Methods for Excited States*; Ferré, N.; Filatov, M.; Huix-Rotllant, M., Eds.; Springer International Publishing: Cham, Switzerland, 2016; Vol. 368, 273–346.
- (43) Liang, Y.; Vinson, J.; Pemmaraju, S.; Drisdell, W. S.; Shirley, E. L.; Prendergast, D. Accurate x-ray spectral predictions: An advanced self-consistent-field approach inspired by many-body perturbation theory. *Phys. Rev. Lett.* **2017**, *118*, 096402.
- (44) Hirata, S.; Head-Gordon, M.; Bartlett, R. J. Configuration interaction singles, time-dependent Hartree–Fock, and time-dependent density functional theory for the electronic excited states of extended systems. *J. Chem. Phys.* **1999**, *111*, 10774–10786.
- (45) Casida, M. E. Time-dependent density-functional theory for molecules and molecular solids. *J. Mol. Struct.: THEOCHEM* **2009**, *914*, 3–18.
- (46) Hunt, W. J.; Goddard, W. A., III Excited states of H₂O using improved virtual orbitals. *Chem. Phys. Lett.* **1969**, *3*, 414–418.
- (47) Huzinaga, S.; Arnau, C. Virtual orbitals in Hartree–Fock theory. *Phys. Rev. A: At, Mol, Opt. Phys.* **1970**, *1*, 1285–1288.
- (48) Huzinaga, S.; Arnau, C. Virtual orbitals in Hartree–Fock theory. II. *J. Chem. Phys.* **1971**, *54*, 1948–1951.
- (49) Morokuma, K.; Iwata, S. Extended Hartree–Fock theory for excited states. *Chem. Phys. Lett.* **1972**, *16*, 192–197.
- (50) Palmieri, P.; Tarroni, R.; Rettrup, S. Hartree–Fock operators to improve virtual orbitals and configuration interaction energies. *J. Chem. Phys.* **1994**, *100*, 5849–5856.
- (51) Potts, D. M.; Taylor, C. M.; Chaudhuri, R. K.; Freed, K. F. The improved virtual orbital-complete active space configuration interaction method, a “packageable” efficient *ab initio* many-body method for describing electronically excited states. *J. Chem. Phys.* **2001**, *114*, 2592–2600.
- (52) Kowalski, K.; Jankowski, K. Towards complete solutions to systems of nonlinear equations of many-electron theories. *Phys. Rev. Lett.* **1998**, *81*, 1195–1198.
- (53) Veeraghavan, S.; Mazziotti, D. A. Global solutions of Hartree–Fock theory and their consequences for strongly correlated quantum systems. *Phys. Rev. A: At, Mol, Opt. Phys.* **2014**, *89*, 010502(R).
- (54) Thom, A. J. W.; Head-Gordon, M. Locating multiple self-consistent field solutions: An approach inspired by metadynamics. *Phys. Rev. Lett.* **2008**, *101*, 193001.
- (55) Hiscock, H. G.; Thom, A. J. W. Holomorphic Hartree–Fock theory and configuration interaction. *J. Chem. Theory Comput.* **2014**, *10*, 4795–4800.
- (56) Thom, A. J. W.; Head-Gordon, M. Hartree–Fock solutions as a quasidiabatic basis for nonorthogonal configuration interaction. *J. Chem. Phys.* **2009**, *131*, 124113.
- (57) Glushkov, V. N.; Wilson, S. Excited state self-consistent field theory using even-tempered primitive Gaussian basis sets. In *Recent Advances in the Theory of Chemical and Physical Systems*; Julien, J.-P., Maruani, J., Mayou, D., Wilson, S., Delgado-Barrio, G., Eds.; Springer: Dordrecht, 2006; Vol. 15, 107–126.
- (58) Glushkov, V. N.; Gidopoulos, N. Constrained optimized potential method and second-order correlation energy for excited states. *Int. J. Quantum Chem.* **2007**, *107*, 2604–2615.
- (59) Glushkov, V. N.; Levy, M. Optimized effective potential method for individual low-lying excited states. *J. Chem. Phys.* **2007**, *126*, 174106.
- (60) Glushkov, V. N.; Wilson, S. Alternative technique for the constrained variational problem based on asymptotic projection method: I. Basics. In *Frontiers in Quantum Systems in Chemistry and Physics. Progress in Theoretical Chemistry and Physics*; 2008, Vol. 18, pp 429–450, DOI: 10.1007/978-1-4020-8707-3_20.
- (61) Glushkov, V. N.; Gidopoulos, N. I.; Wilson, S. Alternative technique for the constrained variational problem based on asymptotic projection method: II. Applications to open-shell self-consistent field theory. In *Frontiers in Quantum Systems in Chemistry and Physics. Progress in Theoretical Chemistry and Physics*; 2008, Vol. 18, pp 451–489, DOI: 10.1007/978-1-4020-8707-3_21.
- (62) Staroverov, V. N.; Glushkov, V. N. Effective local potentials for excited states. *J. Chem. Phys.* **2010**, *133*, 244104.
- (63) Glushkov, V. N. Orthogonality of determinant functions in the Hartree–Fock method for highly excited electronic states. *Opt. Spectrosc.* **2015**, *119*, 1–6.
- (64) Glushkov, V. N.; Assfeld, X. Orthogonality-constrained Hartree–Fock and perturbation theory for high-spin open-shell excited states. *Theor. Chem. Acc.* **2016**, *135*, 3.
- (65) Jacobson, L. D.; Herbert, J. M. A simple algorithm for determining orthogonal, self-consistent excited-state wave functions for a state-specific Hamiltonian: Application to the optical spectrum of the aqueous electron. *J. Chem. Theory Comput.* **2011**, *7*, 2085–2093.

- (66) Cullen, J.; Krykunov, M.; Ziegler, T. The formulation of a self-consistent constricted variational density functional theory for the description of excited states. *Chem. Phys.* **2011**, *391*, 11–18.
- (67) Ziegler, T.; Krykunov, M.; Cullen, J. The implementation of a self-consistent constricted variational density functional theory for the description of excited states. *J. Chem. Phys.* **2012**, *136*, 124107.
- (68) Krykunov, M.; Seth, M.; Ziegler, T. Introducing constricted variational density functional theory in its relaxed self-consistent formulation (RSCF-CV-DFT) as an alternative to adiabatic time dependent density functional theory for studies of charge transfer transitions. *J. Chem. Phys.* **2014**, *140*, 18A502.
- (69) Park, Y. C.; Krykunov, M.; Ziegler, T. On the relation between adiabatic time dependent density functional theory (TDDFT) and the Δ SCF-DFT method. Introducing a numerically stable Δ SCF-DFT scheme for local functionals based on constricted DFT. *Mol. Phys.* **2015**, *113*, 1636–1647.
- (70) Park, Y. C.; Senn, F.; Krykunov, M.; Ziegler, T. Self-consistent constricted variational theory RSCF-CV(∞)-DFT and its restrictions to obtain a numerically stable Δ SCF-DFT-like method: Theory and calculations for triplet states. *J. Chem. Theory Comput.* **2016**, *12*, 5438–5452.
- (71) Senn, F.; Park, Y. C. Constricted variational density functional theory for spatially clearly separated charge-transfer excitations. *J. Chem. Phys.* **2016**, *145*, 244108.
- (72) Evangelista, F. A.; Shushkov, P.; Tully, J. C. Orthogonality constrained density functional theory for electronic excited states. *J. Phys. Chem. A* **2013**, *117*, 7378–7392.
- (73) Derricotte, W. D.; Evangelista, F. A. Simulation of x-ray absorption spectra with orthogonality constrained density functional theory. *Phys. Chem. Chem. Phys.* **2015**, *17*, 14360–14374.
- (74) Verma, P.; Derricotte, W. D.; Evangelista, F. A. Predicting near edge x-ray absorption spectra with the spin-free exact-two-component Hamiltonian and orthogonality constrained density functional theory. *J. Chem. Theory Comput.* **2016**, *12*, 144–156.
- (75) Ramos, P.; Pavanello, M. Low-lying excited states by constrained DFT. *J. Chem. Phys.* **2018**, *148*, 144103.
- (76) Roychoudhury, S.; Sanvito, S.; O'Regan, D. D. Neutral excitation density-functional theory: An efficient and variational first-principles method for simulating neutral excitations in molecules. *Sci. Rep.* **2020**, *10*, 8947.
- (77) Ye, H.-Z.; Welborn, M.; Rieke, N. D.; Van Voorhis, T. σ -SCF: A direct energy-targeting method to mean-field excited states. *J. Chem. Phys.* **2017**, *147*, 214104.
- (78) Ye, H.-Z.; Van Voorhis, T. Half-projected σ self-consistent field for electronic excited states. *J. Chem. Theory Comput.* **2019**, *15*, 2954–2965.
- (79) Zhao, L.; Neuscammann, E. An efficient variational principle for the direct optimization of excited states. *J. Chem. Theory Comput.* **2016**, *12*, 3436–3440.
- (80) Shea, J. A. R.; Neuscammann, E. Communication: A mean field platform for excited state quantum chemistry. *J. Chem. Phys.* **2018**, *149*, 081101.
- (81) Zhao, L.; Neuscammann, E. Density functional extension to excited-state mean-field theory. *J. Chem. Theory Comput.* **2020**, *16*, 164–178.
- (82) Shea, J. A. R.; Gwin, E.; Neuscammann, E. A generalized variational principle with applications to excited state mean field theory. *J. Chem. Theory Comput.* **2020**, *16*, 1526–1540.
- (83) Barca, G. M. J.; Gilbert, A. T. B.; Gill, P. M. W. Excitation number: Characterizing multiply excited states. *J. Chem. Theory Comput.* **2018**, *14*, 9–13.
- (84) Briggs, E. A.; Besley, N. A. Modelling excited states of weakly bound complexes with density functional theory. *Phys. Chem. Chem. Phys.* **2014**, *16*, 14455–14462.
- (85) Lee, J.; Small, D. W.; Head-Gordon, M. Excited states via coupled cluster theory without equation-of-motion methods: Seeking higher roots with application to doubly excited states and double core hole states. *J. Chem. Phys.* **2019**, *151*, 214103.
- (86) Levi, G.; Ivanov, A. V.; Jonsson, H. Variational calculations of excited states via direct optimization of orbitals in DFT. *Faraday Discuss.* **2020**, DOI: 10.1039/D0FD00064G.
- (87) Kowalczyk, T.; Yost, S. R.; Van Voorhis, T. Δ SCF density functional theory approach for electronic excitations in organic dyes. *J. Chem. Phys.* **2011**, *134*, 054128.
- (88) Briggs, E. A.; Besley, N. A.; Robinson, D. QM/MM excited state molecular dynamics and fluorescence spectroscopy of BODIPY. *J. Phys. Chem. A* **2013**, *117*, 2644–2650.
- (89) Hanson-Heine, M. W. D.; George, M. W.; Besley, N. A. Calculating excited state properties using Kohn-Sham density functional theory. *J. Chem. Phys.* **2013**, *138*, 064101.
- (90) Besley, N. A. Theoretical study of electronically excited states. *AIP Conf. Proc.* **2014**, *1618*, 576–584.
- (91) Hanson-Heine, M. W. D.; Wriglesworth, A.; Uroos, M.; Calladine, J. A.; Murphy, T. S.; Hamilton, M.; Clark, I. P.; Towrie, M.; Dowden, J.; Besley, N. A.; George, M. W. Calculating singlet excited states: Comparison with fast time-resolved infrared spectroscopy of coumarins. *J. Chem. Phys.* **2015**, *142*, 154119.
- (92) Suess, C. J.; Hirst, J. D.; Besley, N. A. Quantum chemical calculations of tryptophan \rightarrow heme electron and excitation energy transfer rates in myoglobin. *J. Comput. Chem.* **2017**, *38*, 1495–1502.
- (93) Hanson-Heine, M. W. D.; Calladine, J. A.; Yang, J.; Towrie, M.; Horvath, R.; Besley, N. A.; George, M. W. A combined time-resolved infrared and density functional theory study of the lowest excited states of 9-fluorenone and 2-naphthaldehyde. *Chem. Phys.* **2018**, *512*, 44–52.
- (94) Besley, N. A.; Gilbert, A. T. B.; Gill, P. M. W. Self-consistent-field calculations of core excited states. *J. Chem. Phys.* **2009**, *130*, 124308.
- (95) Michelitsch, G. S.; Reuter, K. Efficient simulation of near-edge x-ray absorption fine structure (NEXAFS) in density-functional theory: Comparison of core-level constraining approaches. *J. Chem. Phys.* **2019**, *150*, 074104.
- (96) Ambroise, M. A.; Jensen, F. Probing basis set requirements for calculating core ionization and core excitation spectroscopy by the Δ self-consistent-field approach. *J. Chem. Theory Comput.* **2019**, *15*, 325–337.
- (97) Northey, T.; Norell, J.; Fouda, A. E. A.; Besley, N. A.; Odelius, M.; Penfold, T. J. Ultrafast nonadiabatic dynamics probed by nitrogen K-edge absorption spectroscopy. *Phys. Chem. Chem. Phys.* **2020**, *22*, 2667–2676.
- (98) Ehlert, C.; Klamroth, T. PSIXAS: A Psi4 plugin for efficient simulations of x-ray absorption spectra based on the transition-potential and Δ -Kohn–Sham method. *J. Comput. Chem.* **2020**, *41*, 1781–1789.
- (99) Imamura, Y.; Nakai, H. Description of core-ionized and core-excited states by density functional theory and time-dependent density functional theory. In *Quantum Systems in Chemistry and Physics*; Nishikawa, K., Maruani, J., Brändas, E. J., Delgado-Barrio, G., Piecuch, P., Eds.; Springer Science+Business Media: Dordrecht, 2012; Vol. 26, 275–308, .
- (100) Tolbatov, I.; Chipman, D. M. Comparative study of Gaussian basis sets for calculation of core electron binding energies in first-row hydrides and glycine. *Theor. Chem. Acc.* **2014**, *133*, 1560.
- (101) Tolbatov, I.; Chipman, D. M. Benchmarking density functionals and Gaussian basis sets for calculation of core-electron binding energies in amino acids. *Theor. Chem. Acc.* **2017**, *136*, 82.
- (102) Cabral do Couto, P.; Hollas, D.; Slavíček, P. On the performance of optimally tuned range-separated hybrid functionals for x-ray absorption modeling. *J. Chem. Theory Comput.* **2015**, *11*, 3234–3244.
- (103) Coons, M. P.; Herbert, J. M. Quantum chemistry in arbitrary dielectric environments: Theory and implementation of nonequilibrium Poisson boundary conditions and application to compute vertical ionization energies at the air/water interface. *J. Chem. Phys.* **2018**, *148*, 222834; Erratum: **2019**, *151*, 189901.
- (104) Hanson-Heine, M. W. D.; George, M. W.; Besley, N. A. Basis sets for the calculation of core-electron binding energies. *Chem. Phys. Lett.* **2018**, *699*, 279–285.

- (105) Hanson-Heine, M. W. D.; George, M. W.; Besley, N. A. A scaled CIS(D) based method for the calculation of valence and core electron ionization energies. *J. Chem. Phys.* **2019**, *151*, 034104.
- (106) Besley, N. A. Equation of motion coupled cluster theory calculations of the x-ray emission spectroscopy of water. *Chem. Phys. Lett.* **2012**, *542*, 42–46.
- (107) Wadey, J. D.; Besley, N. A. Quantum chemical calculations of x-ray emission spectroscopy. *J. Chem. Theory Comput.* **2014**, *10*, 4557–4564.
- (108) Hanson-Heine, M. W. D.; George, M. W.; Besley, N. A. Kohn-Sham density functional theory calculations of non-resonant and resonant x-ray emission spectroscopy. *J. Chem. Phys.* **2017**, *146*, 094106.
- (109) Zhovtobriukh, I.; Besley, N. A.; Fransson, T.; Nilsson, A.; Petterson, L. G. M. Relationship between x-ray emission and absorption spectroscopy and the local H-bond environment in water. *J. Chem. Phys.* **2018**, *148*, 144507.
- (110) Clarke, C. J.; Hayama, S.; Hawes, A.; Hallett, J. P.; Chamberlain, T. W.; Lovelock, K. R. J.; Besley, N. A. Zinc 1s valence-to-core x-ray emission spectroscopy of halozincate complexes. *J. Phys. Chem. A* **2019**, *123*, 9552–9559.
- (111) Zhang, Y.; Mukamel, S.; Khalil, M.; Govind, N. Simulating valence-to-core x-ray emission spectroscopy of transition metal complexes with time-dependent density functional theory. *J. Chem. Theory Comput.* **2015**, *11*, 5804–5809.
- (112) Zhang, Y.; Bergmann, U.; Schoenlein, R.; Khalil, M.; Govind, N. Double core hole valence-to-core x-ray emission spectroscopy: A theoretical exploration using time-dependent density functional theory. *J. Chem. Phys.* **2019**, *151*, 144114.
- (113) Holden, W. M.; Jahrman, E. P.; Govind, N.; Seidler, G. T. Probing sulfur chemical and electronic structure with experimental observation and quantitative theoretical prediction of $K\alpha$ and valence-to-core $K\beta$ x-ray emission spectroscopy. *J. Phys. Chem. A* **2020**, *124*, 5415–5434.
- (114) Van Voorhis, T.; Head-Gordon, M. A geometric approach to direct minimization. *Mol. Phys.* **2002**, *100*, 1713–1721.
- (115) Richings, G. W.; Karadakov, P. B. Improved convergence of Hartree-Fock style excited-state wavefunctions using second-order optimization with an exact Hessian. *Theor. Chem. Acc.* **2013**, *132*, 1400.
- (116) Peng, B.; Van Kuiken, B. E.; Ding, F.; Li, X. A guided self-consistent-field method for excited state wave function optimization: Applications to ligand-field transitions in transition-metal complexes. *J. Chem. Theory Comput.* **2013**, *9*, 3933–3938.
- (117) Garza, A. J.; Scuseria, G. E. Comparison of self-consistent field convergence acceleration techniques. *J. Chem. Phys.* **2012**, *137*, 054110.
- (118) Mewes, J.-M.; Jovanovic, V.; Marian, C. M.; Dreuw, A. On the molecular mechanism of non-radiative decay of nitrobenzene and the unforeseen challenges this simple molecule holds for electronic structure theory. *Phys. Chem. Chem. Phys.* **2014**, *16*, 12393–12406.
- (119) Hait, D.; Head-Gordon, M. Excited state orbital optimization via minimizing the square of the gradient: General approach and application to singly and doubly excited states via density functional theory. *J. Chem. Theory Comput.* **2020**, *16*, 1699–1710.
- (120) McIver, J. W., Jr.; Komornicki, A. Structure of transition states in organic reactions. General theory and an application to the cyclobutene-butadiene isomerization using a semiempirical molecular orbital method. *J. Am. Chem. Soc.* **1972**, *94*, 2625–2633.
- (121) Angelani, L.; Di Leonardo, R.; Ruocco, G.; Scala, A.; Sciortino, F. Saddles in the energy landscape probed by supercooled liquids. *Phys. Rev. Lett.* **2000**, *85*, 5356–5359.
- (122) Angelani, L.; Di Leonardo, R.; Ruocco, G.; Scala, A.; Sciortino, F. Quasisaddles as relevant points of the potential energy surface in dynamics of supercooled liquids. *J. Chem. Phys.* **2002**, *116*, 10297–10306.
- (123) Doye, J. P. K.; Wales, D. J. Saddle points and dynamics of Lennard-Jones clusters, solids, and supercooled liquids. *J. Chem. Phys.* **2002**, *116*, 3777–3788.
- (124) Szabo, A.; Ostlund, N. *S. Modern Quantum Chemistry*; Macmillan: New York, 1982.
- (125) Doye, J. P. K.; Wales, D. J. Comment on “Quasisaddles as relevant points of the potential energy surface in the dynamics of supercooled liquids. *J. Chem. Phys.* **2003**, *118*, 5263–5264.
- (126) Saunders, V. R.; Hillier, I. H. A “level-shifting” method for converging closed shell Hartree-Fock wave functions. *Int. J. Quantum Chem.* **1973**, *7*, 699–705.
- (127) Salek, P.; Høst, S.; Thøgersen, L.; Jørgensen, P.; Manninen, P.; Olsen, J.; Jansík, B.; Reine, S.; Pawłowski, F.; Tellgren, E.; Helgaker, T.; Coriani, S. Linear-scaling implementation of molecular electronic self-consistent field theory. *J. Chem. Phys.* **2007**, *126*, 114110.
- (128) Cancès, E.; Le Bris, C. On the convergence of SCF algorithms for the Hartree-Fock equations. *ESAIM: Math. Modell. Numer. Anal.* **2000**, *34*, 749–774.
- (129) Høst, S.; Olsen, J.; Jansík, B.; Thøgersen, L.; Jørgensen, P.; Helgaker, T. The augmented Roothaan–Hall method for optimizing Hartree–Fock and Kohn-Sham density matrices. *J. Chem. Phys.* **2008**, *129*, 124106.
- (130) Thøgersen, L.; Olsen, J.; Köhn, A.; Jørgensen, P. The trust-region self-consistent field method in Kohn-Sham density-functional theory. *J. Chem. Phys.* **2005**, *123*, 074103.
- (131) Martin, R. L. Natural transition orbitals. *J. Chem. Phys.* **2003**, *118*, 4775–4777.
- (132) Surján, P. R. Natural orbitals in CIS and singular-value decomposition. *Chem. Phys. Lett.* **2007**, *439*, 393–394.
- (133) Ziegler, T.; Rauk, A.; Baerends, E. J. On the calculation of multiplet energies by the Hartree-Fock-Slater method. *Theor. Chem. Acc.* **1977**, *43*, 261–271.
- (134) Daul, C. Density functional theory applied to the excited states of coordination compounds. *Int. J. Quantum Chem.* **1994**, *52*, 867–877.
- (135) Kitagawa, Y.; Saito, T.; Ito, M.; Shoji, M.; Koizumi, K.; Yamanaka, S.; Kawakami, T.; Okumura, M.; Yamaguchi, K. Approximately spin-projected geometry optimization method and its application to di-chromium systems. *Chem. Phys. Lett.* **2007**, *442*, 445–450.
- (136) Nair, N. N.; Schreiner, E.; Pollet, R.; Staemmler, V.; Marx, D. Magnetostructural dynamics with the extended broken symmetry formalism: Antiferromagnetic [2Fe-2S] complexes. *J. Chem. Theory Comput.* **2008**, *4*, 1174–1188.
- (137) Thompson, L. M.; Hratchian, H. P. On approximate projection models. *Mol. Phys.* **2019**, *117*, 1421–1429.
- (138) Frank, I.; Hutter, J.; Marx, D.; Parrinello, M. Molecular dynamics in low-spin excited states. *J. Chem. Phys.* **1998**, *108*, 4060–4069.
- (139) Briggs, E. A.; Besley, N. A. Density functional theory based analysis of photoinduced electron transfer in a triazacryptand based K^+ sensor. *J. Phys. Chem. A* **2015**, *119*, 2902–2907.
- (140) Jiao, L.; Yu, C.; Wang, J.; Briggs, E. A.; Besley, N. A.; Robinson, D.; Ruedas-Rama, M. J.; Orte, A.; Crovetto, L.; Talavera, E. M.; Alvarez-Pez, J. M.; Van der Auweraer, M.; Boens, N. Unusual spectroscopic and photophysical properties of *meso-tert-butyl*BODIPY in comparison to related alkylated BODIPY dyes. *RSC Adv.* **2015**, *5*, 89375–89388.
- (141) Kowalczyk, T.; Le, K.; Irle, S. Self-consistent optimization of excited states within density-functional tight-binding. *J. Chem. Theory Comput.* **2016**, *12*, 313–323.
- (142) Yamaguchi, K.; Jensen, F.; Dorigo, A.; Houk, K. N. A spin correction procedure for unrestricted Hartree-Fock and Møller-Plesset wavefunctions for singlet diradicals and polyradicals. *Chem. Phys. Lett.* **1988**, *149*, 537–542.
- (143) Shao, Y.; et al. Advances in molecular quantum chemistry contained in the Q-Chem 4 program package. *Mol. Phys.* **2015**, *113*, 184–215.
- (144) Robin, M. R. *Higher Excited States of Polyatomic Molecules*; Academic Press: New York, 1985; Vol. III, DOI: 10.1016/B978-0-12-589903-1.X5001-2.
- (145) Loos, P.-F.; Boggio-Pasqua, M.; Scemama, A.; Caffarel, M.; Jacquemin, D. Reference energies for double excitations. *J. Chem. Theory Comput.* **2019**, *15*, 1939–1956.
- (146) Loos, P.-F.; Scemama, A.; Blondel, A.; Garniron, Y.; Caffarel, M.; Jacquemin, D. A mountaineering strategy to excited states: Highly

accurate reference energies and benchmarks. *J. Chem. Theory Comput.* **2018**, *14*, 4360–4379.

(147) Mardirossian, N.; Head-Gordon, M. ω B97X-V: A 10-parameter, range-separated hybrid, generalized gradient approximation density functional with nonlocal correlation, designed by a survival-of-the-fittest strategy. *Phys. Chem. Chem. Phys.* **2014**, *16*, 9904–9924.

(148) Perdew, J. P.; Schmidt, K. Jacob's ladder of density functional approximations for the exchange-correlation energy. In *Density Functional Theory and Its Applications to Materials*; Van Doren, V. E., Van Alsenoy, C., Geerlings, P., Eds.; American Institute of Physics: 2001; Vol. 577, 1–20.

(149) Mardirossian, N.; Head-Gordon, M. Mapping the genome of meta-generalized gradient approximation density functionals: The search for B97M-V. *J. Chem. Phys.* **2015**, *142*, 074111.

(150) Becke, A. D. Density-functional thermochemistry. III. The role of exact exchange. *J. Chem. Phys.* **1993**, *98*, 5648–5652.

(151) Lee, C.; Yang, W.; Parr, R. G. Development of the Colle-Salvetti correlation-energy formula into a functional of the electron density. *Phys. Rev. B: Condens. Matter Mater. Phys.* **1988**, *37*, 785–789.

(152) Becke, A. D. Density-functional exchange-energy approximation with correct asymptotic behavior. *Phys. Rev. A: At., Mol., Opt. Phys.* **1988**, *38*, 3098–3100.

(153) Head-Gordon, M.; Rico, R. J.; Oumi, M.; Lee, T. J. A doubles correction to electronic excited states from configuration interaction in the space of single substitutions. *Chem. Phys. Lett.* **1994**, *219*, 21–29.

(154) van Leeuwen, R.; Baerends, E. J. Exchange-correlation potential with correct asymptotic behavior. *Phys. Rev. A: At., Mol., Opt. Phys.* **1994**, *49*, 2421–2431.

(155) Casida, M. E.; Jamorski, C.; Casida, K. C.; Salahub, D. R. Molecular excitation energies to high-lying bound states from time-dependent density-functional response theory: Characterization and correction of the time-dependent local density approximation ionization threshold. *J. Chem. Phys.* **1998**, *108*, 4439–4439.

(156) Tozer, D. J.; Handy, N. C. Improving virtual Kohn–Sham orbitals and eigenvalues: Application to excitation energies and static polarizabilities. *J. Chem. Phys.* **1998**, *109*, 10180–10189.

(157) Tozer, D. J.; Amos, R. D.; Handy, N. C.; Roos, B. O.; Serrano-Andrés, L. Does density functional theory contribute to the understanding of excited states of unsaturated organic compounds? *Mol. Phys.* **1999**, *97*, 859–868.

(158) Ralps, K.; Serna, G.; Hargreaves, L. R.; Khakoo, M. A.; Winstead, C.; McKoy, V. Excitation of the six lowest electronic transitions in water by 9–20 eV electrons. *J. Phys. B: At., Mol. Opt. Phys.* **2013**, *46*, 125201.

(159) Weigend, F.; Ahlrichs, R. Balanced basis sets of split valence, triple zeta valence and quadruple zeta valence quality for H to Rn: Design and assessment of accuracy. *Phys. Chem. Chem. Phys.* **2005**, *7*, 3297–3305.

(160) Hellweg, A.; Rappoport, D. Development of new auxiliary basis functions of the Karlsruhe segmented contracted basis sets including diffuse basis functions (def2-SVPD, def2-TZVPPD, and def2-QVPPD) for RI-MP2 and RI-CC calculations. *Phys. Chem. Chem. Phys.* **2015**, *17*, 1010–1017.

(161) Grimme, S. Improved second-order Møller–Plesset perturbation theory by separate scaling of parallel- and antiparallel-spin pair correlation energies. *J. Chem. Phys.* **2003**, *118*, 9095–9102.

(162) Jung, Y.; Lochan, R. C.; Dutoi, A. D.; Head-Gordon, M. Scaled opposite-spin second order Møller–Plesset correlation energy: An economical electronic structure method. *J. Chem. Phys.* **2004**, *121*, 9793–9802.

(163) Lochan, R. C.; Jung, Y.; Head-Gordon, M. Scaled opposite spin second order Møller–Plesset theory with improved physical description of long-range dispersion interactions. *J. Phys. Chem. A* **2005**, *109*, 7598–7605.

(164) Thierbach, A.; Neiss, C.; Gallandi, L.; Marom, N.; Körzdörfer, T.; Görling, A. Accurate valence ionization energies from Kohn–Sham eigenvalues with the help of potential adjusters. *J. Chem. Theory Comput.* **2017**, *13*, 4726–4740.

(165) Besley, N. A.; Peach, M. J. G.; Tozer, D. J. Time-dependent density functional theory calculations of near-edge x-ray absorption fine structure with short-range corrected functionals. *Phys. Chem. Chem. Phys.* **2009**, *11*, 10350–10358.

(166) Besley, N. A.; Asmuruf, F. A. Time-dependent density functional theory calculations of the spectroscopy of core electrons. *Phys. Chem. Chem. Phys.* **2010**, *12*, 12024–12039.

(167) Norman, P.; Dreuw, A. Simulating x-ray spectroscopies and calculating core-excited states of molecules. *Chem. Rev.* **2018**, *118*, 7208–7248.

(168) Brundle, C. R.; Robin, M. B.; Kuebler, N. A.; Basch, H. Perfluoro effect in photoelectron spectroscopy. I. Nonaromatic molecules. *J. Am. Chem. Soc.* **1972**, *94*, 1451–1465.

(169) Winter, B.; Weber, R.; Widdra, W.; Dittman, M.; Faubel, M.; Hertel, I. V. Full valence band photoemission from liquid water using EUV synchrotron radiation. *J. Phys. Chem. A* **2004**, *108*, 2625–2632.

(170) Woon, D. E.; Dunning, T. H., Jr. Gaussian basis sets for use in correlated molecular calculations. V. Core-valence basis sets for boron through neon. *J. Chem. Phys.* **1995**, *103*, 4572–4585.

(171) Peterson, K. A.; Dunning, T. H., Jr. Accurate correlation consistent basis sets for molecular core–valence correlation effects: The second row atoms Al–Ar, and the first row atoms B–Ne revisited. *J. Chem. Phys.* **2002**, *117*, 10548.

(172) Hait, D.; Head-Gordon, M. Highly accurate prediction of core spectra of molecules at density functional theory cost: Attaining sub-electronvolt error from a restricted open-shell Kohn–Sham approach. *J. Phys. Chem. Lett.* **2020**, *11*, 775–786.

(173) Fadley, C. S. X-ray photoelectron spectroscopy: Progress and perspectives. *J. Electron Spectrosc. Relat. Phenom.* **2010**, *178–179*, 2–32.

(174) Bagus, P. S.; Ilton, E. S.; Nelin, C. J. The interpretation of XPS spectra: Insights into materials properties. *Surf. Sci. Rep.* **2013**, *68*, 273–304.

(175) Pueyo Bellafont, N.; Saiz, G. A.; Viñes, F.; Illas, F. Performance of Minnesota functionals on predicting core-level binding energies of molecules containing main-group elements. *Theor. Chem. Acc.* **2016**, *135*, 35.

(176) Olivieri, G.; Goel, A.; Kleibert, A.; Cvetko, D.; Brown, M. A. Quantitative ionization energies and work functions of aqueous solutions. *Phys. Chem. Chem. Phys.* **2016**, *18*, 29506–29515.

(177) Takahata, Y.; Chong, D. P. DFT calculation of core-electron binding energies. *J. Electron Spectrosc. Relat. Phenom.* **2003**, *133*, 69–76.

(178) Lloyd, D. R.; Lynaugh, N. Photoelectron studies of boron compounds I. Diborane, borazine and B-trifluoroborazine. *Philos. Trans. R. Soc., A* **1970**, *268*, 97–109.

(179) Gouterman, M.; Wagnière, G. H.; Snyder, L. C. Spectra of porphyrins: Part II. Four orbital model. *J. Mol. Spectrosc.* **1963**, *11*, 108–127.

(180) Stockett, M. H.; Musbat, L.; Kjær, C.; Houmøller, J.; Toker, Y.; Rubio, A.; Milne, B. F.; Nielsen, S. B. The Soret absorption band of isolated chlorophyll *a* and *b* tagged with quaternary ammonium ions. *Phys. Chem. Chem. Phys.* **2015**, *17*, 25793–25798.

(181) Milne, B. F.; Toker, Y.; Rubio, A.; Nielsen, S. B. Unraveling the intrinsic color of chlorophyll. *Angew. Chem., Int. Ed.* **2015**, *54*, 2170–2173.

(182) Linnanto, J.; Korppi-Tommola, J. Quantum chemical simulation of excited states of chlorophylls, bacteriochlorophylls and their complexes. *Phys. Chem. Chem. Phys.* **2006**, *8*, 663–687.

(183) Hay, P. J.; Shavitt, I. *Ab initio* configuration interaction studies of the π -electron states of benzene. *J. Chem. Phys.* **1974**, *60*, 2865–2877.

(184) Ziegler, L. D.; Hudson, B. S. The vibronic spectroscopy of benzene: Old problems and new techniques. In *Excited States*; Lim, E. C., Ed.; Elsevier: 1982; Vol. 5, 41–140, DOI: 10.1016/B978-0-12-227205-9.50007-6.

(185) Sun, J.; Ruzsinszky, A.; Perdew, J. P. Strongly constrained and appropriately normed semilocal density functional. *Phys. Rev. Lett.* **2015**, *115*, 036402.

(186) Yanai, T.; Tew, D. P.; Handy, N. C. A new hybrid exchange–correlation functional using the Coulomb–attenuating method (CAM-B3LYP). *Chem. Phys. Lett.* **2004**, *393*, 51–57.

(187) Ohio Supercomputer Center. <http://osc.edu/ark:/19495/f5s1ph73> (accessed 2020-07-20).